Engineering 24 (2023) 21–38

Contents lists available at ScienceDirect

Engineering

journal homepage: www.elsevier.com/locate/eng

Research
Micro and Nano Manipulation and Characterization—Review

Selective and Independent Control of Microrobots in a Magnetic Field: A Review

Min Wang [a], Tianyi Wu [a], Rui Liu [a], Zhuoran Zhang [b,*], Jun Liu [a,c,*]

[a] Department of Mechanical Engineering, City University of Hong Kong, Hong Kong 999077, China
[b] School of Science and Engineering, The Chinese University of Hong Kong (Shenzhen), Shenzhen 518057, China
[c] Shenzhen Research Institutes of City University of Hong Kong, Shenzhen 518057, China

ARTICLE INFO

Article history:
Received 16 August 2021
Revised 18 September 2022
Accepted 9 February 2023
Available online 14 April 2023

Keywords:
Microrobot
Magnetic microrobot
Independent control
Selective control
Microrobotic manipulation

ABSTRACT

Due to the unique advantages of untethered connections and a high level of safety, magnetic actuation is a commonly used technique in microrobotics for propelling microswimmers, manipulating fluidics, and navigating medical devices. However, the microrobots or actuated targets are exposed to identical and homogeneous driving magnetic fields, which makes it challenging to selectively control a single robot or a specific group among multiple targets. This paper reviews recent advances in selective and independent control for multi-microrobot or multi-joint microrobot systems driven by magnetic fields. These selective and independent control approaches decode the global magnetic field into specific configurations for the individualized actuation of multiple microrobots. The methods include applying distinct properties for each microrobot or creating heterogeneous magnetic fields at different locations. Independent control of the selected targets enables the effective cooperation of multiple microrobots to accomplish more complicated operations. In this review, we provide a unique perspective to explain how to manipulate individual microrobots to achieve a high level of group intelligence on a small scale, which could help accelerate the translational development of microrobotic technology for real-life applications.

1. Introduction

Robotic manipulation using a magnetic field has shown significant progress in the past couple of decades and has made a profound impact in a variety of applications, such as microrobots biopsy [1], drug delivery [2], cell manipulation [3], and microassembly [4]. In magnetic manipulations, microrobots that are built with permanent magnets or ferromagnetic materials are actuated wirelessly by means of external magnetic fields. Compared with other manipulation strategies, such as acoustic [5], optical [6], thermal [7], and piezoelectric approaches [8], magnetic actuation has intrinsic advantages in terms of its untethered connection, large force output, and high level of safety.

In a typical magnetic microrobotic system, single or multiple robots made of ferromagnetic materials [9–11] are actuated inside the workspace of an external programmable magnetic field. The external field is generated and controlled by magnetic coils with a controllable current or by permanent magnets with adjustable positions [12,13]. The microrobots are moved by magnetic forces or torques using gradient or uniform magnetic fields. However, actuation methods driven by a global field suffer from low flexibility in the control of multiple microrobots, because the movement of a selected robot or agent inevitably affects other objects in the workspace. Therefore, the cooperative control of multiple or a swarm of microrobots has been studied to achieve complicated micromanipulation tasks [14,15]. In addition to swarm manipulation, the selective and independent control of a single agent within a group is a challenging yet useful methodology for cooperative micromanipulation in order to achieve complicated group tasks.

This paper describes the fundamentals of magnetic micromanipulation, reviews existing selective and independent control methods for multiple microrobots, and discusses potential applications and future research. Unlike other review topics in this field, such as the motion principle and control [16,17], advanced applications [18,19], and biohybrid actuation [20], this paper focuses on the independent and selective control of individual magnetic

* Corresponding authors.
E-mail addresses: zhangzhuoran@cuhk.edu.cn (Z. Zhang), Jun.Liu@cityu.edu.hk (J. Liu).

https://doi.org/10.1016/j.eng.2023.02.011

robots in a multiple robot system. The selective control of field-driven microrobots is of great importance in increasing the operation speed, expanding the load capabilities of microrobots, and improving the flexibility of collaborative manipulation. With these advances, magnetic microrobots will be enabled to achieve broad applications with a higher level of intelligence.

This review describes the fundamental actuation mechanisms for magnetic microrobots and summarizes different control strategies for the selective manipulation of these devices. Mainstream independent control strategies can be divided into five categories, as shown in Fig. 1: ① global uniform field strategies, which rely on an individual's differing torque response in a global rotational uniform field; ② global gradient field strategies, in which an unequal magnetic force is caused by a non-uniform gradient field; ③ local moveable magnet strategies, in which an enhanced local magnetic field is generated by moveable magnets; ④ local electromagnet strategies, which rely on selective activation via addressable planar magnetic coils; and ⑤ frequency resonate strategies that rely on the differential resonance of individual microrobots. Combinations of these strategies have also been reported in the literature.

This review is organized as follows. Section 2 introduces the magnetic actuation mechanism, including the generation of magnetic force, magnetic torque, and the coupling effect with controlled devices. The five categories of advanced independent control strategies are summarized in Section 3. After that, Section 4 describes state-of-the-art applications using independent control strategies. Section 5 discusses the potential and future perspectives of the independent control approach in a multiple robot system, which is followed by a conclusion in Section 6.

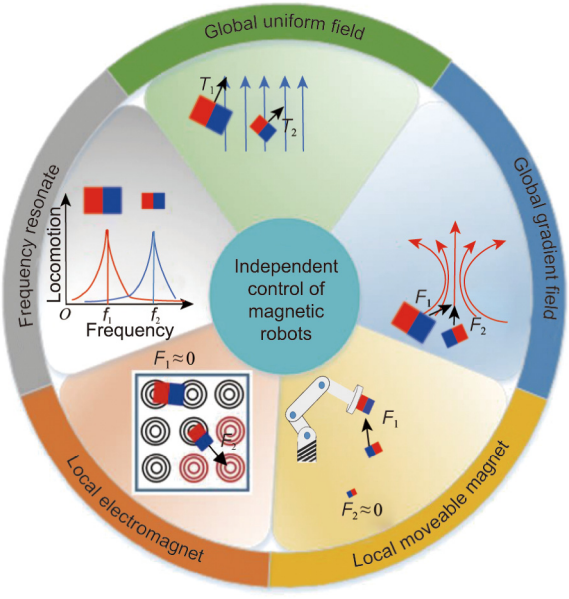

Fig. 1. Independent control strategies for multiple magnetic robot systems can be categorized into five categories, explained clockwise beginning from the top. Global uniform field: Magnetic robots are designed with different characteristics or a limited rotation angle and are actuated by a uniform field. Global gradient field: A global gradient field is applied to generate a location-dependent force mapping control. Local moveable magnet: An external permanent magnet is used to enhance the local magnetic density. Local electromagnet: Selective actuation is performed via a planar coil array. Frequency resonates: Magnetic robots are designed with a distinct resonate frequency and actuated by an external frequency-variable magnetic field. F_1, F_2: magnetic force on individuals; f_1, f_2: applied actuation frequency; T_1, T_2: magnetic torque on individuals.

2. Principles of magnetic manipulation

Magnetic actuation relies on the coupling of externally applied magnetic fields and magnetic individuals. To better understand the fundamental mechanism of magnetic actuation, this section introduces how an external magnetic field is generated from two typical magnetic sources: permanent magnets and electromagnets. We also investigate in detail why varying an external field can be used to manipulate a micro individual. Overall, the locomotion of magnetic robots is affected by the coupled magnetic torque, force, and interaction between individuals.

2.1. Magnetic field generation

Compared with magnetic field generated from energized coils, a permanent magnet is an energy-friendly and highly efficient material for manipulating small objects. In addition, a permanent magnet occupies less space than electromagnetic coils to produce the same level of magnetic field. The major limitation of permanent magnet-based methods is that the magnetic strength cannot be turned off after operation. The magnetic strength exerted on a controlled device is dependent on the source's magnetic moment $\boldsymbol{M}$, volume V, and source-to-devices vector $\boldsymbol{r}$. When the source-devices distance is much larger than the dimension of the magnetic source, the dipole model can be used to express the distribution of the magnetic field.

$$\boldsymbol{B}\{\boldsymbol{M}, V, \boldsymbol{r}\} = \left(\frac{\mu_0}{4\pi \boldsymbol{r}^5}\left(3\boldsymbol{r}\boldsymbol{r}^{\mathrm{T}} - \boldsymbol{r}^2\boldsymbol{I}\right)\right)V\boldsymbol{M} \tag{1}$$

where $\boldsymbol{B}\{\boldsymbol{M}, V, \boldsymbol{r}\}$ is the magnetic field generated by the dipole magnet; μ_0 is the air permeability; and $\boldsymbol{I}$ is the identity matrix.

According to Eq. (1), the magnetic strength decays cubically with distance and is proportional to the volume and magnetic moment of the magnetic source. After the magnetic source is selected, one can adjust the orientation and position of the source magnet to generate a desired magnetic flux density at the location of the controlled microrobot.

Electromagnetic coils are the other way to generate an adjustable magnetic field. Unlike permanent magnets, electromagnetic coils can change the field strength without moving the magnetic sources, providing a more controllable solution for magnetic actuation. As a magnetic source, electromagnetic coils suffer from a relatively low magnetic force and torque in comparison with permanent magnets. Possible solutions to increase the force and torque output include using a large current or increasing the number of coils. However, these solutions can raise concerns about the increased heat generation and energy costs. Two typical settings for electromagnetic systems are the Helmholtz coil and the Maxwell coil, which can provide a uniform field and a gradient field, respectively. Without loss of generality, the magnetic field of a cylindrical coil can be determined using the Biot–Savart Law, as follows:

$$\boldsymbol{B}\{i, h, \boldsymbol{r}, \boldsymbol{l}, N\} = \frac{N\mu_0 i}{4\pi}\int_h \int_{\boldsymbol{l}} \frac{\mathrm{d}\boldsymbol{l} \times \boldsymbol{r}}{\boldsymbol{r}^3}\mathrm{d}h \tag{2}$$

where N is the number of coil layers; i is the current density; $\boldsymbol{l}$ is the unit vector of the coil; and h is the height of the coil.

After an electromagnetic system is built with a fixed size and a constant number of coils, the magnetic strength at a given point (i.e., at the location of the controlled device) is dependent on the energized current of the position and the orientation of the cylindrical coil. To increase the flexibility of electromagnetic systems, researchers have designed moveable coils to perform more complex tasks and minimize energy consumption [21,22].

2.2. Actuation mechanism of a magnetic microrobot

In magnetic manipulation, microrobots are fabricated using magnetic materials that can be excited by external magnetic induction. Magnetic materials are classified into soft and hard magnetic materials, according to the coercive force and magnetic resistance. Soft magnets have relatively low magnetization (i.e., coercivity < 1000 $A{\cdot}m^{-1}$), whereas hard magnetic materials have a higher magnetic strength that is usually considered to be constant under an external actuation magnetic field. For simplicity in this discussion, the following sections analyze the actuation mechanism of the magnetized material using a constant magnetic moment, $\boldsymbol{M}$. More details on the magnetization process are provided in Refs. [16,18].

2.2.1. Magnetic torque

When a magnetic dipole is used to generate an external magnetic field $\boldsymbol{B}$, the controlled devices tend to align and rotate with the external magnetic field. A rotational field makes the controlled device follow the rotation because of the changing magnetic torque. The general form of the magnetic torque on a controlled magnetic device can be expressed as follows:

$$\boldsymbol{T} = \boldsymbol{B} \times \boldsymbol{M} \tag{3}$$

where $\boldsymbol{M} = [M_x M_y M_z]^{\mathrm{T}}$ and $\boldsymbol{B} = [B_x B_y B_z]^{\mathrm{T}}$ are the dipole moment and applied field in each axis, respectively. According to Eq. (3), the devices or microrobots are rotated by the torque generated from the changing magnetic field $\boldsymbol{B}$. In microrobotic applications, a helical or screw-like structure is widely adopted to transform the rotary motion into a linear motion for moving the controlled device in the workspace.

2.2.2. Magnetic force

The gradient of the magnetic field causes the force that acts on the magnetic devices. At the location with a magnetic gradient $\nabla \boldsymbol{B}$, the general form of the magnetic force exerted on a controlled device with a magnetic moment $\boldsymbol{M}$ can be expressed as follows:

$$\boldsymbol{F} = (\boldsymbol{M} \cdot \nabla)\boldsymbol{B} = \left(M_x \frac{\partial}{\partial x} + M_y \frac{\partial}{\partial y} + M_z \frac{\partial}{\partial z}\right)\boldsymbol{B} \tag{4}$$

From this equation, the magnetic force is proportional to the magnetic moment of the controlled devices, which is a function of the object size and the magnetization strength. When a uniform magnetic field is applied (i.e., $\frac{\partial \boldsymbol{B}}{\partial x} = \frac{\partial \boldsymbol{B}}{\partial y} = \frac{\partial \boldsymbol{B}}{\partial z} = 0$), no force is generated on the controlled devices.

2.2.3. Magnetic interactions between individuals

When multiple microrobots are present in the workspace and are close to each other, the interactions among them can significantly affect their behaviors. Since the amplitude of the external magnetic field is much higher than that of the local field generated from the controlled microrobots, the controlled devices are more likely to align with the external magnetic field. However, because of the short distance between two neighboring microrobots, the local interaction force is not negligible [18,23].

Without the loss of generality, the following discussion uses two controlled devices (R_1 and R_2) as an example. As shown in Fig. 2, the transition between repulsion and attraction can be controlled by changing the direction of the external magnetic field. With the fixed magnetic moments ($\boldsymbol{M}_1$ and $\boldsymbol{M}_2$), the force on the R_1 generated by the magnetic source R_2 can be expressed by substituting Eq. (1) into Eq. (4). Here, the R_1 with a magnetic moment $\boldsymbol{M}_1$ is regarded as the field-generating unit and the R_2 with a magnetic moment $\boldsymbol{M}_2$ is regarded as the force-receiving unit. By substituting the magnetic field at position R_2 (generated by R_1) into Eq. (4), the corresponding magnetic interaction force is

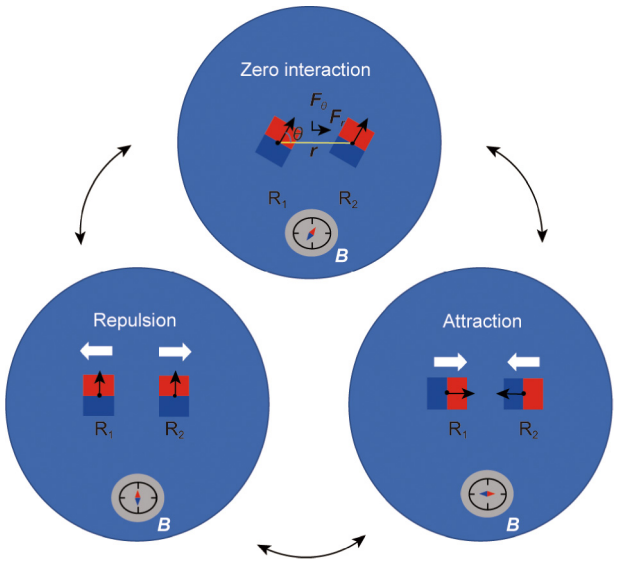

Fig. 2. The interaction between two magnetic devices. By adjusting the direction of the external magnetic field, the interaction of two magnetic substances can be converted from repulsion to attraction. θ: the angle between the global magnetic field direction and the connecting line (R_1–R_2) of two controlled devices; $\boldsymbol{F}_r$, $\boldsymbol{F}_\theta$: the forces along and perpendicular to the connecting line, respectively.

$$\boldsymbol{F} = -\nabla\left(\frac{\mu_0}{4\pi\|\boldsymbol{r}\|^3}\left(\boldsymbol{M}_1 \cdot \boldsymbol{M}_2 - 3\frac{(\boldsymbol{M}_1 \cdot \boldsymbol{r})(\boldsymbol{M}_2 \cdot \boldsymbol{r})}{\|\boldsymbol{r}\|^2}\right)\right) \tag{5}$$

Given the angle θ between the global magnetic field direction and the connecting line (R_1–R_2) of two controlled devices (shown in Fig. 2), the interaction force in Eq. (5) can be rewritten as follows:

$$\boldsymbol{F} = -\frac{\mu_0 \boldsymbol{M}_1 \boldsymbol{M}_2}{4\pi}\nabla\left(\frac{1 - 3\cos^2\theta}{\|\boldsymbol{r}\|^3}\right) \tag{6}$$

Using the cylindrical coordinate system, the interaction force can be decoupled into two components, $\boldsymbol{F}_r$ and $\boldsymbol{F}_\theta$, which respectively denote the forces along and perpendicular to the connecting line.

$$\boldsymbol{F}_r = \frac{3\mu_0 \boldsymbol{M}_1 \boldsymbol{M}_2 (1 - 3\cos^2\theta)}{4\pi\|\boldsymbol{r}\|^4} \tag{7}$$

$$\boldsymbol{F}_\theta = \frac{3\mu_0 \boldsymbol{M}_1 \boldsymbol{M}_2 (2\cos\theta\sin\theta)}{4\pi\|\boldsymbol{r}\|^4} \tag{8}$$

If we let $\boldsymbol{F}_r = 0$, then the critical angle $\theta = 54.73°$ is solved. When the angle is smaller than the critical value, the two microrobots are attracted to each other. When the angle is larger than the critical value, the microrobots repulse each other. The force $\boldsymbol{F}_\theta$ indicates the rotational tendency of clockwise or counterclockwise, which is utilized during swarm control to generate vortexes or aligned patterns in order to arrange magnetic particles [24,25]. Other researchers have also used the interaction force to control the distance between devices for logistic tasks [26,27].

3. Advanced control strategies

Compared with single and swarm robot systems, the multi-robot systems that can be independently controlled permit the completion of complex collaboration tasks with high efficiency.

With the development of micro/nano fabrication techniques and advances in control strategies, various approaches have been employed for the selective control of magnetic robots in a multi-agent system. As mentioned earlier, these strategies can be roughly divided into five categories. We review these five kinds of methodologies and summarize their advantages and limitations in this section.

3.1. Global uniform field strategies

It is challenging to control each microrobot independently in a multi-microrobot system, because all microrobots receive the same driving signals from the external magnetic field. Methods to achieve nonidentical behaviors must be developed to break the homogeneity among individual magnetic robots. This section reviews three types of independent control methods in a uniform magnetic field: individualized design with different geometry or a distinct magnetic moment, activating or locking individuals via magnetic hysteretic characteristics, and applying auxiliary structures to limit unnecessary degrees of freedoms (DoFs).

A global uniform field can be generated by a Helmholtz coil, which is the commonly used method to output a uniform field. However, fabricating the small robot with different properties is a nontrivial task, and designing novel structures at a small scale to limit unnecessary DoFs is also a challenge.

3.1.1. Distinct magnetic properties

The selective control of multiple microrobots in a homogeneous field can be achieved by differentiating the design of each microrobot. Changing the fabrication materials and geometries enables independent control of individuals, because different materials have various responses to a uniform magnetic field. Moreover, geometrical differences require distinct torque for rotation.

Fig. 3(a) [28–30] shows the independent control approaches by designing individuals with distinct inner physical properties. To locomote a magnetic target on the ground using a unique external magnetic field $\boldsymbol{B}$, the magnetization of the target should surpass the threshold valve $\boldsymbol{M}_{\min}$ to overcome the gravitational torque T_g of the target. Floyd et al. [28] used $\boldsymbol{M}_{\min}$ as the threshold value to selectively actuate microrobots made of soft and hard magnetic materials. When the applied magnetic field was not strong enough

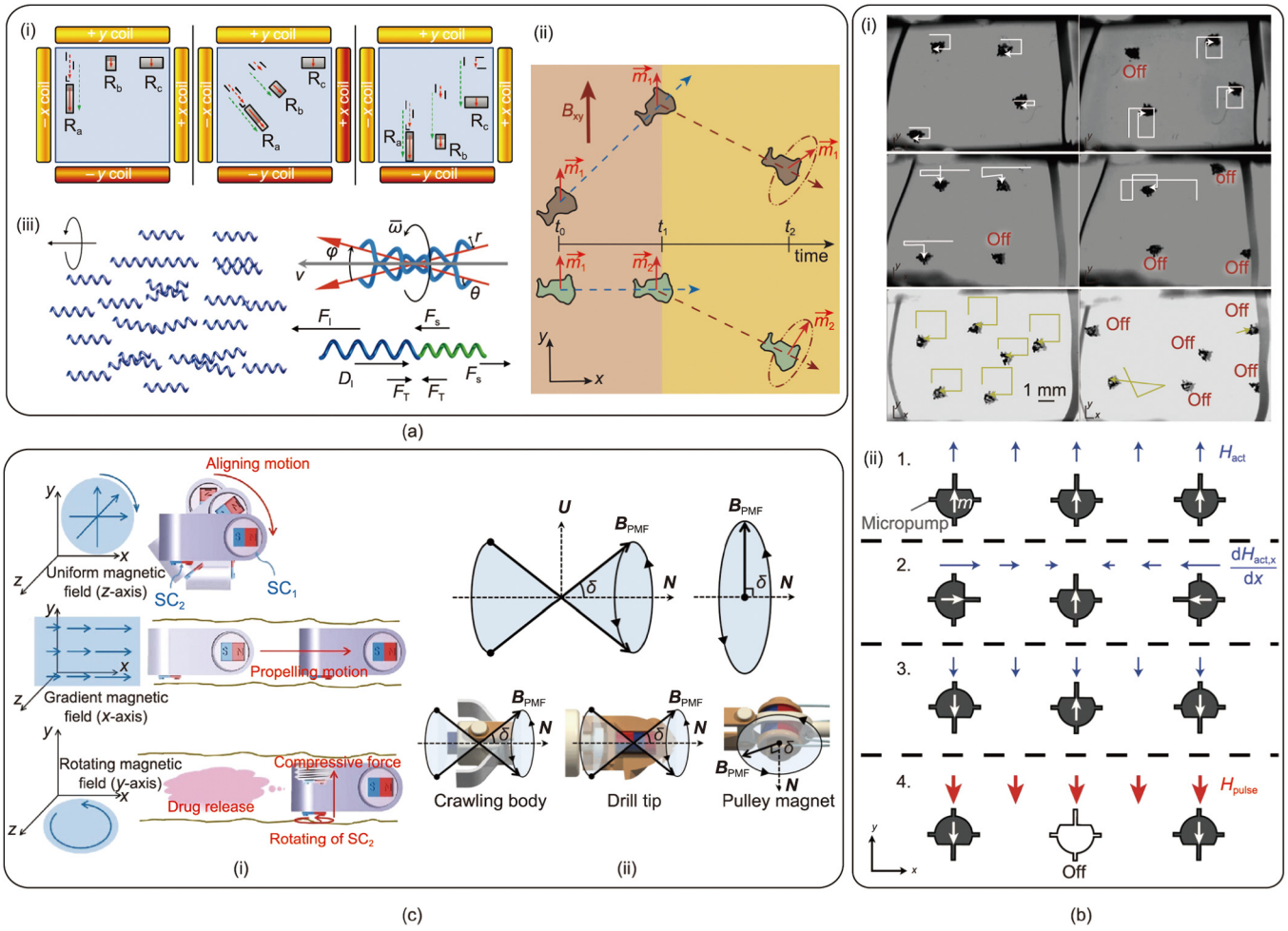

Fig. 3. Independent locomotion under a homogeneous field. (a) Distinct inner physical properties for selective control: (i) different manufacturing materials and sizes; (ii) the uniform field changes the devices' orientation and gradient field to propel the devices; (iii) a helical robot with different diameters and lengths. (b) Hysteresis characteristics for selective control: (i) controlled devices with different coercivity; (ii) controlled devices with the same materials but different magnetization directions. (c) Special structural design to limit certain DoFs: (i) capsule endoscope with two orthogonal chambers; (ii) crowing robot with independent crow, drill, and pulley structure. R_a, R_b, R_c: robots; $\overrightarrow{m_1}$, $\overrightarrow{m_2}$: a pair of nanostructures at arbitrary locations with respect to each other; t_0, t_1, t_2: time; B_{xy}: external applied direct current (DC) field; ϖ: angular velocity; r: radius; φ: assembly angle; θ: helix angle; v: swimming velocity; F_l, F_s: propulsion forces of swimmers l and s; F_T: towing force; D_l, D_s: drag of swimmers l and s; m: magnetic moment; H_{act}: magnetic actuation field; H_{pulse}: magnetization switching field pulse; SC_1, SC_2: screw caps; δ: precession angle; $\boldsymbol{B}_{PMF}$: precession magnetic field ($0 < \delta < 90°$); $\boldsymbol{B}_{RMF}$: rotating magnetic field ($\delta = 90°$); $\boldsymbol{N}$: a unit vector of the rotating axis; $\boldsymbol{U}$: a unit vector normal to the $\boldsymbol{N}$. (a) Reproduced from Refs. [28–30] with permission; (b) reproduced from Refs. [33,34] with permission; (c) reproduced from Refs. [35,36] with permission.

to magnetize the soft magnetic material to reach the threshold value, only the hard magnetic microrobot was selected to locomote. In contrast, soft and hard magnets can be actuated simultaneously if the applied field is higher than $\boldsymbol{M}_{\min}$. In this way, both soft and hard materials can be magnetized ((i) in Fig. 3(a)) [28]. A decoupling mechanism was also reported on multi-nanomotors with identical shapes but different magnetization directions. In this system, micromotors with unique body orientations can align with a uniform field. By oscillating the constant field, different microrobots can be made to rock with different axes and translate to separated destinations. As a result, by programming the constant and oscillating field, direction and positioning control can be achieved independently ((ii) in Fig. 3(a)) [29].

Moreover, microrobots made of the same materials with various aspect ratios were utilized for independent control according to their separate rotational inertias [31]. A robot with a high aspect ratio has a large rotation inertia and a low angular acceleration when actuated by an oscillating field. For example, if the angular velocity is low, the microrobots can rotate around the contact points. In contrast, if the angular velocity is too fast to be followed by the microrobots, the contact point may slip on the surface. In a subsequent study, the researchers extended the parallel locomotion to two-dimensional (2D) independent control by varying the velocity response of each microrobot with distinct control signals [32]. Similarly, Tottori et al. [30] achieved the selective control of three magnetic microrobots by changing the length of a helical structure. This method was applied to rearrange the microrobots for an assembly process ((iii) in Fig. 3(a)).

3.1.2. Magnetic hysteretic variations

The magnetic hysteretic curve reveals the remanence level of magnetic materials during a magnetization or demagnetization process. The robot with not the same materials has a different hysteresis, which can be used for the selective control via the distinct magnetic coactivity and remanence. For microrobots made of the same material, the hysteretic characteristics do not change. However, the magnetization effect in different directions contributes differently to a microrobot with asymmetric geometry. For example, the long axis of an elliptical individual is easier to magnetize than the short axis, which can be used for selective actuation by utilizing orientation differences among microrobots. Diller et al. [33] demonstrated independent control via selective magnetization and demagnetization for microrobots made of both the same and different materials ((i) in Fig. 3(b)). The experimental results showed that a group of microrobots could move independently. This approach is expected to be effective for microrobots of different sizes, as long as they have distinct magnetic hysteretic properties. A similar approach was adopted for microfluidic applications ((ii) in Fig. 3(b)) [34]. In this system, several pumps made of neodymium-iron-boron and ferrite particles could be selectively turned on or off by a strong external pulse field when the pumps were adjusted to different orientations.

3.1.3. Novel physical structure design

In general, magnetic microrobots with the same design have identical responses to a uniform magnetic field in an unconstrained workspace. To allow differentiated movements and diverse functions in each joint, novel mechanical designs have been proposed that limit part of the DoFs and permit individualized actuation. A representative design proposed by Choi et al. [35] is a capsule microrobot for drug delivery ((i) in Fig. 3(c)). This microrobot contains two orthogonal cylindrical chambers that can be selectively actuated by rotating the magnetic screw caps. After the capsule microrobot is moved to the lesion under a gradient field, two chambers can be selectively released through a uniform rotational magnetic field with a different rotation axis. In another study, Lee et al. [36] proposed a magnetically pulled robot working in a tubular environment. The robot was able to crawl in narrow tubular surroundings and could drill or expand to unclog blocked regions ((ii) in Fig. 3(c)). This independent joint control was achieved by orthogonally placing a joint control magnet. In this way, different functions such as crawling or drilling can be achieved.

3.2. Global gradient field strategies

As discussed in Section 3.1, differential torque-based actuation requires individuals made through difficult fabrication processes or built with extra structures to limit coupled DoFs. These methods have limitations, such as time cost, energy waste, and room occupation. Solutions using a gradient field for actuation have been proposed, which can simplify the fabrication process for the independent control of microrobots with the same physical properties. This section summarizes advances in selective control involving different magnetic forces generated by gradient fields. In a non-uniform field, the magnetic gradient can be controlled to achieve the effect of different forces on a robot at several positions. Therefore, this approach requires real-time position feedback and kinematic modeling for each microrobot. Based on whether the number of inputs is more than the required DoFs, gradient-based independent control systems are divided into fully actuated and underactuated systems [37]. For example, when more than one particle is present, the utilized system has only one control input (e.g., a permanent magnet or coil), and more than one DoF needs to be controlled. Hence, the system is defined as underactuated. Fig. 4 [21,37–44] shows some representative studies for independent controlling individuals by fully actuated and under actuated systems, respectively.

3.2.1. Fully actuated system

When the number of control inputs is equal to or greater than the product of the controllable robots with their operable DoFs, the magnetic actuation system is defined as fully actuated. In this case, the kinematics and controlling matrix are relatively easy to model, as no other additional force needs to be included in the equations. Nevertheless, the required coils increase with the number of controllable targets, so this method can only control a small number of magnetic targets due to the limited space.

Independent control of two magnetic targets using gradient fields was first demonstrated in a one-DoF scenario ((i) in Fig. 4(a)) [38]. In this work, two coils were installed on two sides of a tube, and two robots were placed in the tube. The net force for one of these robots was the superposition of the external magnetic force and the interaction force between two microrobots. Accordingly, one microrobot could be selectively actuated while the other was kept stationary with a zero net force. With position feedback, the selective control of two magnets was achieved in both an open- and closed-loop manner. To expand the workspace into a 2D plane, Wong et al. [39] designed a magnetic system with four stationary coils to move two identical robots independently. First, they mapped the force–position relationship based on the numerical simulation and an analytical study. Then, the researchers created waypoints with predefined velocity and acceleration for each microrobot ((ii) in Fig. 4(a)) [39]. Real-time vision feedback was uploaded to the proportion–integration–differentiation (PID) controller for trajectory following and close loop control. The experimental results showed that the two magnetic robots were controlled following their trajectory in an 85 mm diameter petri dish with a tracking error of less than 1.5 mm.

Denasi and Misra [45] proposed a leader–follower control scheme for manipulating two magnetic microrobots. The researchers improved the dynamic modeling accuracy by including the

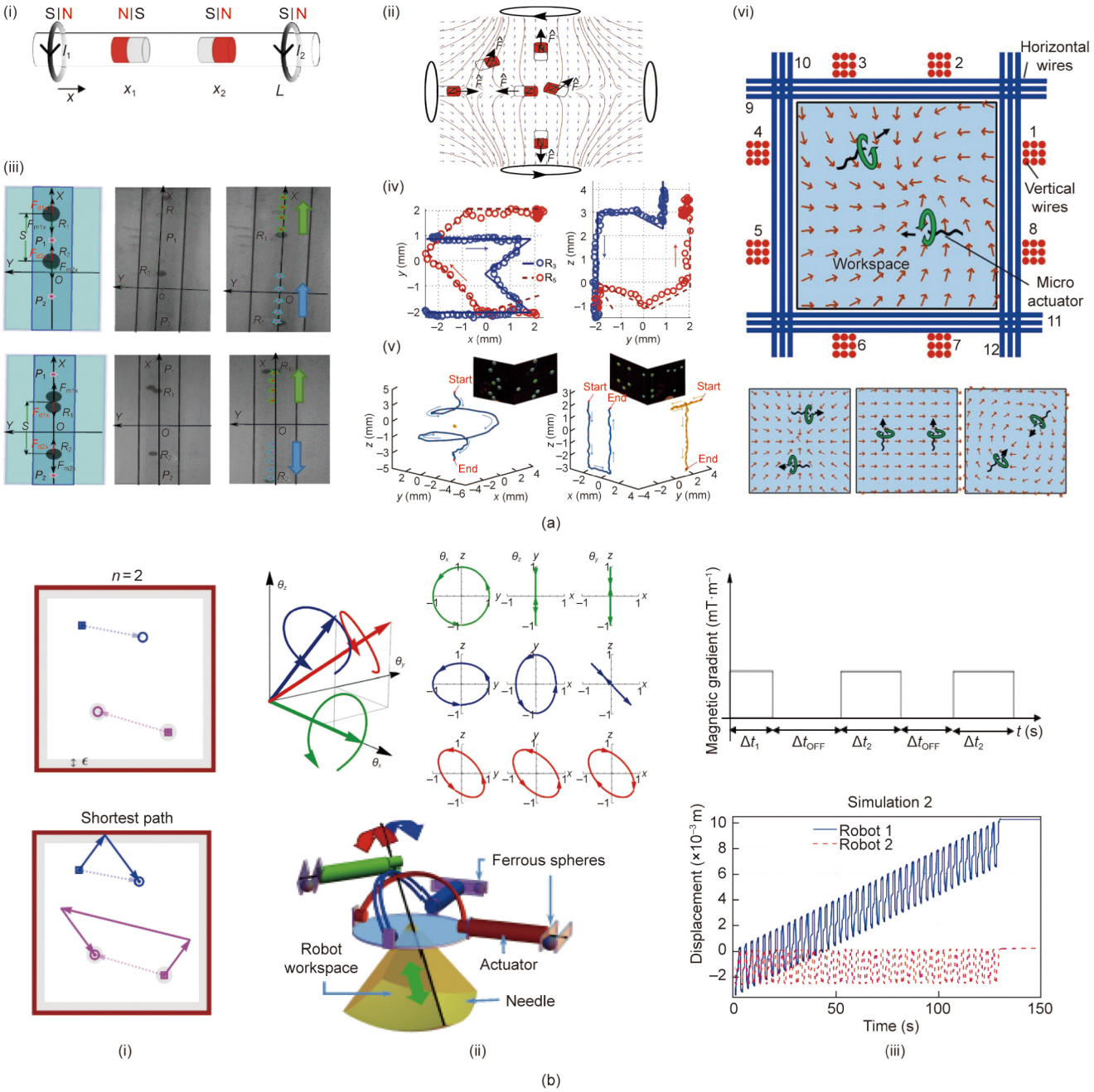

Fig. 4. Independent manipulation based on a gradient field. (a) Fully actuated system: (i) selective control of two magnetic robots in a 1D pipeline; (ii) controllable movement of two magnetic particles in a 2D plane; (iii) controllable locomotion of two microrobots in the same and opposite direction; (iv) two controlled devices move with independent trajectories in 3D space; (v) two magnetic beads can be controlled independently or can move along different trajectories simultaneously; (vi) customized multiple sets of coils drive two targets, of which eight sets of coils are arranged vertically, and four sets of coils are arranged in a plane. (b) Underactuated system: (i) combined with a sidewall effect to realize independent position control; (ii) combined with inertial transients via the designed width and sequence of the magnetic field; (iii) customized structure to limit the DoFs in unrequired directions. I_1, I_2: current through coil; x_1, x_2: position; L: distance between coils; $\widehat{F}$: orientation and force vector; R_1, R_2: radius of microbeads; P_1, P_2: final position; F_{d1x}, F_{d2x}: drag forces; F_{m1x}, F_{m2x}: magnetic force; S: initial distance separating the microbeads; R_3, R_5: microrobots with different shape; n: number of DoF; ε: the minimum spacing between two robots and the minimum separation from the boundaries; θ_x, θ_y, θ_z: rotational angle with different axis; Δt_1, Δt_2: the width of a sequence of pulses; Δt_{OFF}: a zero input of duration. (a) Reproduced from Refs. [21,38–42] with permission; (b) reproduced from Refs. [37,43,44] with permission.

magnetic force, hydrodynamic drag force, buoyancy force, and gravitational force. With the accurate dynamic model, the two microrobots were actuated to follow a preset trajectory with an average error of about 10 mm. Mellal et al. [40] improved systems' accuracy by adopting linear quadratic controller to move multiple magnetic microbeads at different velocities in the same or opposite directions ((iii) in Fig. 4(a)). In some applications, microrobots are required to move in a 3D space. Diller et al. [41] achieved the independent actuation of multiple magnetic microrobots in 3D space ((iv) in Fig. 4(a)). Ongaro et al. [21] developed more dexterous actuation systems by integrating moveable electromagnetic coils to levitate and translocate multiple microrobots in a fluidic environment ((v) in Fig. 4(a)). The systems were designed to produce a high magnetic gradient and to maintain the balance between gravity and magnetic force. Using a similar strategy, researchers developed a new electromagnetic system by integrating eight

vertical coils to generate a tunable magnetic field in the *X*- and *Y*-directions and four horizontal coils to control the magnetic strength in the *Z*-direction ((vi) in Fig. 4(a)) [42].

3.2.2. Underactuated system

Because of the limited workspace, most applications do not have sufficient magnetic sources to selectively actuate multiple individuals. For example, clinical application always requires more than one robot for cooperative tasks, while only one magnetic source (e.g., magnetic resonance imaging (MRI)) exists in a clinical operating room. Thus, external forces other than magnetic force should be involved in actuation. Solutions have been proposed in recent years, such as combining magnetic force with adhesion force generated by sidewalls, adopting the interaction force between individuals, adding friction via the mechanical structure, and so forth. In 2017, Shahrokhi et al. [43] achieved the independent position control of two homogeneous particles using magnetic force and sidewall friction ((i) in Fig. 4(b)). Because of the adhesion force, the particle near the sidewall was locked, while the other particle could be actuated freely under a magnetic field. With the assistance of the sidewall interaction, the two particles could be moved to different positions. The particle that interacted with the sidewall was moved using a shortest-path algorithm, whereas the freely moving particle was programmed to compensate for the movement, allowing both particles to reach the destination simultaneously ((i) in Fig. 4(b)) [43]. Two years later, the researchers expanded the workspace from a square space to a convex region, and the system was upgraded to 3D position-independent control by introducing the gravity force into the dynamic model [46].

Independent control can also be achieved in an underactuated system by means of a unique mechanical design. In Ref. [44], the system contained three orthogonal pivots, and a ferrous sphere was installed at the end of the pivots. The magnetic field at a given point could be decoupled into three directions ((ii) in Fig. 4(b)) [44]. If the applied force was parallel to the pivot axis, no torque was generated, and the corresponding axis was kept fixed without any rotation. Adopting this mechanism, the researchers demonstrated the control of a magnetic device for targeted delivery and biopsy by a commercial MRI.

Without assistance from the surroundings, it is challenging to achieve independent control of multiple microrobots in an underactuated system, because the motion of multiple microrobots is nonlinear in a gradient field. Researchers have attempted to tackle this limitation using the perspective of control strategies. For example, Vartholomeos et al. [37] achieved independent position control of two millimeter-scale magnetic robots using a gradient field with programmable pulse widths. As shown in (iii) in Fig. 4(b) [37], in one cycle, one of the robots could be controlled to be in a dynamic equilibrium state, with a net displacement of zero. The other robot could be actuated toward the destination. In a subsequent study, the same group introduced a robust and stable controller with optimal switching between actuation and tracking for the independent closed-loop control of two magnetic robots [47].

3.2.3. Actuation by uniform and gradient field

A rotational uniform magnetic field and a gradient field are used to actuate magnetic microrobots through magnetic torque and force, respectively. Accordingly, a rotational field actuates a microrobot with rotational movement, while a gradient field actuates a microrobot with translational movement. This section discusses selective control methods that employ a combination of a uniform field and a gradient field. In this actuation framework, one of the actuation modes (torque or force) is utilized to lock the unselected targets, while the other drive mode is responsible for operating the other targets. This selective control framework is inspired by magnetostatic bacteria whose moving direction is governed by a magnetic field, while kinetic energy is responsible for moving the bacteria forward as the power source [48]. Two independently actuated magnetic particles were demonstrated to move sequentially or in a parallel manner using a combined rotational and gradient field. For sequential movement control (Fig. 5(a)) [49], the unselected microswimmer is locked in place through a dynamic balance between rotational propelling and drag force. Because the rotational axis of the uniform field is perpendicular to the direction of the gradient, movement along the rotation axis is restricted. For simultaneous movement control, it is challenging to actuate two individuals to locomote toward the desired directions using a gradient field. The researchers proposed a step-by-step method to actuate two individuals simultaneously. To improve the control precision, the gradient field was adjusted once the distance between the swimmers and their desired positions was larger than the threshold value.

Rahmer et al. [50] reported an approach for the spatially selective actuation of helical micromachines. In this study, the researchers installed three magnetic rings on screws distributed in the workspace. The applied field was the combination of a static gradient field $\boldsymbol{H}_{\mathrm{s}}$, a rotational field for field-free point selecting $\boldsymbol{H}_{\mathrm{offs}}$, and a uniform rotational field for actuation $\boldsymbol{H}_{\mathrm{rot}}$, shown as: $\boldsymbol{H} = \boldsymbol{H}_{\mathrm{s}} + \boldsymbol{H}_{\mathrm{offs}} + \boldsymbol{H}_{\mathrm{rot}}$. A magnetic field-free point was created via the offset of a static gradient field $\boldsymbol{H}_{\mathrm{s}}$ and a uniform offset field $\boldsymbol{H}_{\mathrm{offs}}$. A rotational uniform field $\boldsymbol{H}_{\mathrm{rot}}$ was adopted for rotating the magnetic target. In contrast, the magnetic rings at other points were locked because of the friction between the rings and screws (Fig. 5(b)) [50].

In 2015, Petruska and Nelson [51] proved that a magnetic field and its gradient could be modeled as eight independent components at any point in the workspace. Three years later, Salmanipour and Diller [52] demonstrated the independent control of up to eight DoFs with a maximum coupling of 8.6%. As shown in Fig. 5(c) [52], the eight-DoF magnetic system involves seven cubic magnets that are physically constrained to experience deflections along one or two axes. The external magnetic field and its gradient can produce various combinations of a force and torque element on each agent for independent control. Similarly, other researchers developed a multifunctional capsule robot with seven DoFs that can be independently actuated, as shown in Fig. 5(d) [53]. Three DoFs were used to control the drag chamber for spray, and the other DoFs were designed for locomotion and biopsy. The experimental results showed that the average crosstalk error among the DoFs was 7.0%, with the highest error of 18.3%. Recently, two magnetic microgrippers were proposed to independently pick up and deliver cargo to two separate destinations with a path planner algorithm, where an external gradient magnetic field was used to adjust the position of the two grippers. When the grippers were moved close to objects, the precision locations were adjusted by the interaction force between individuals (Fig. 5(e)) [27].

3.3. Local electromagnet strategies

The methods discussed in previous sections are based on global magnetic field input. The input current of each magnetic coil is precisely controlled to enable the movement of selected magnetic microrobots, while minimizing the coupling for other microrobots. Therefore, the control algorithms involve complex modeling with a high order of control matrix, and the trajectory error can easily accumulate if no feedback is provided, because the actuating effects of the unselected target cannot be eliminated. To simplify the control problem, researchers have developed specialized substrates that can produce a localized magnetic field for actuation. The manipulation mechanism of such systems typically uses embedded micro solenoids or electrostatic pads to propel or anchor the selected microrobots. Fig. 6 [4,54–65] summarizes the

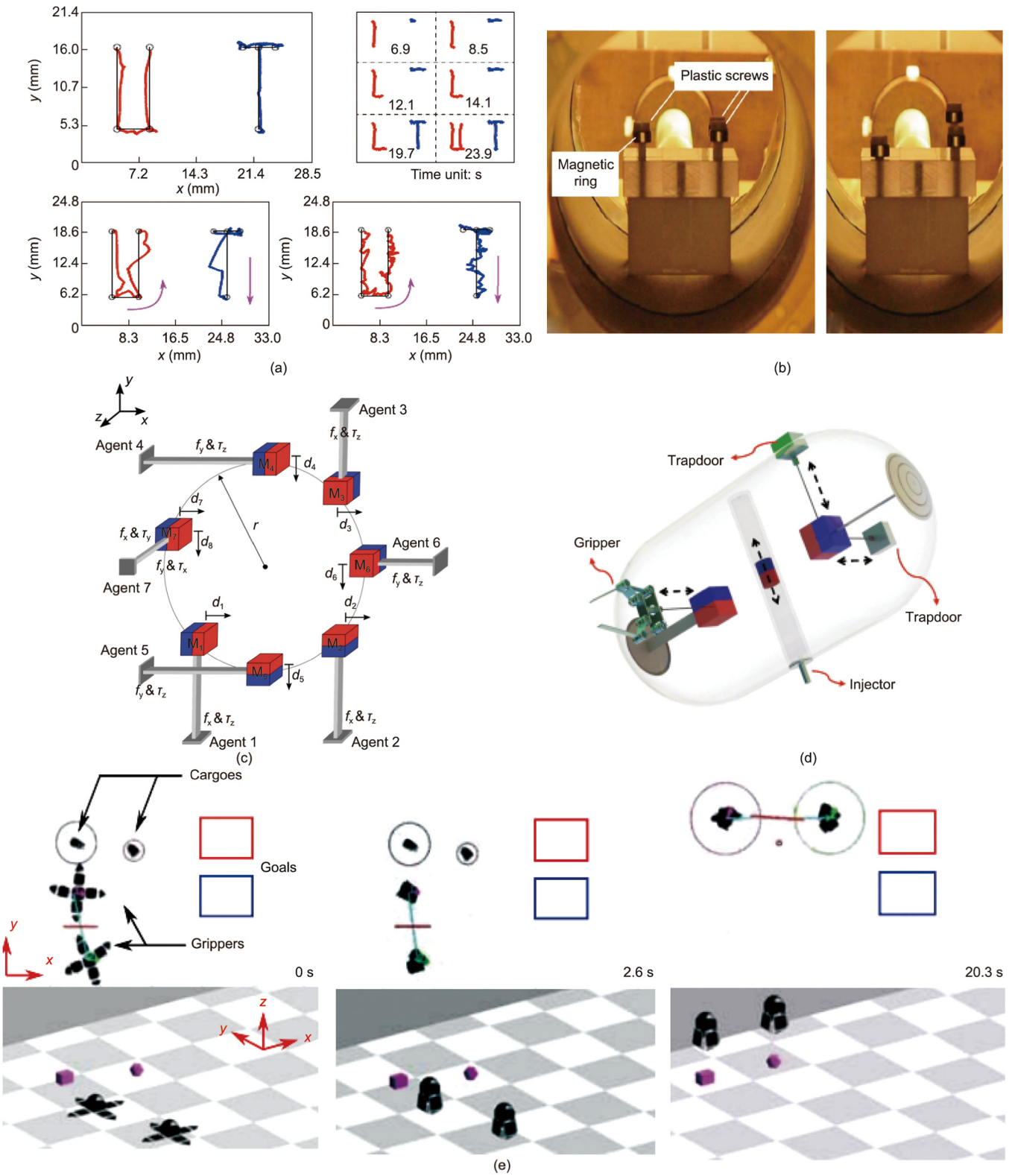

Fig. 5. Use of a combined uniform field and gradient field to manipulate individuals independently. (a) A uniform field is adopted to activate the device; then, the robot is dragged by the gradient field. (b) The gradient field improves the pressure between helical machines and screws, thereby increasing the friction force; then, the rotational uniform field actuates the robot up and down. (c) Independent control of eight DoFs is achieved using gradient and uniform magnetic fields. (d) A capsule robot with independent control for drug delivery and biopsy. (e) Rotating a uniform magnetic field changes the attitude of the controlled devices, thereby adjusting their interaction to achieve independent position control; then, a gradient magnetic field is used to transfer cargo. d_1–d_8: moving direction; f_x, f_y: actuation force; τ_x, τ_y, τ_z: actuation torque; M_1–M_7: magnets. (a) Reproduced from Ref. [49] with permission; (b) reproduced from Ref. [50] with permission; (c) reproduced from Ref. [52] with permission; (d) reproduced from Ref. [53] with permission; (e) reproduced from Ref. [27] with permission.

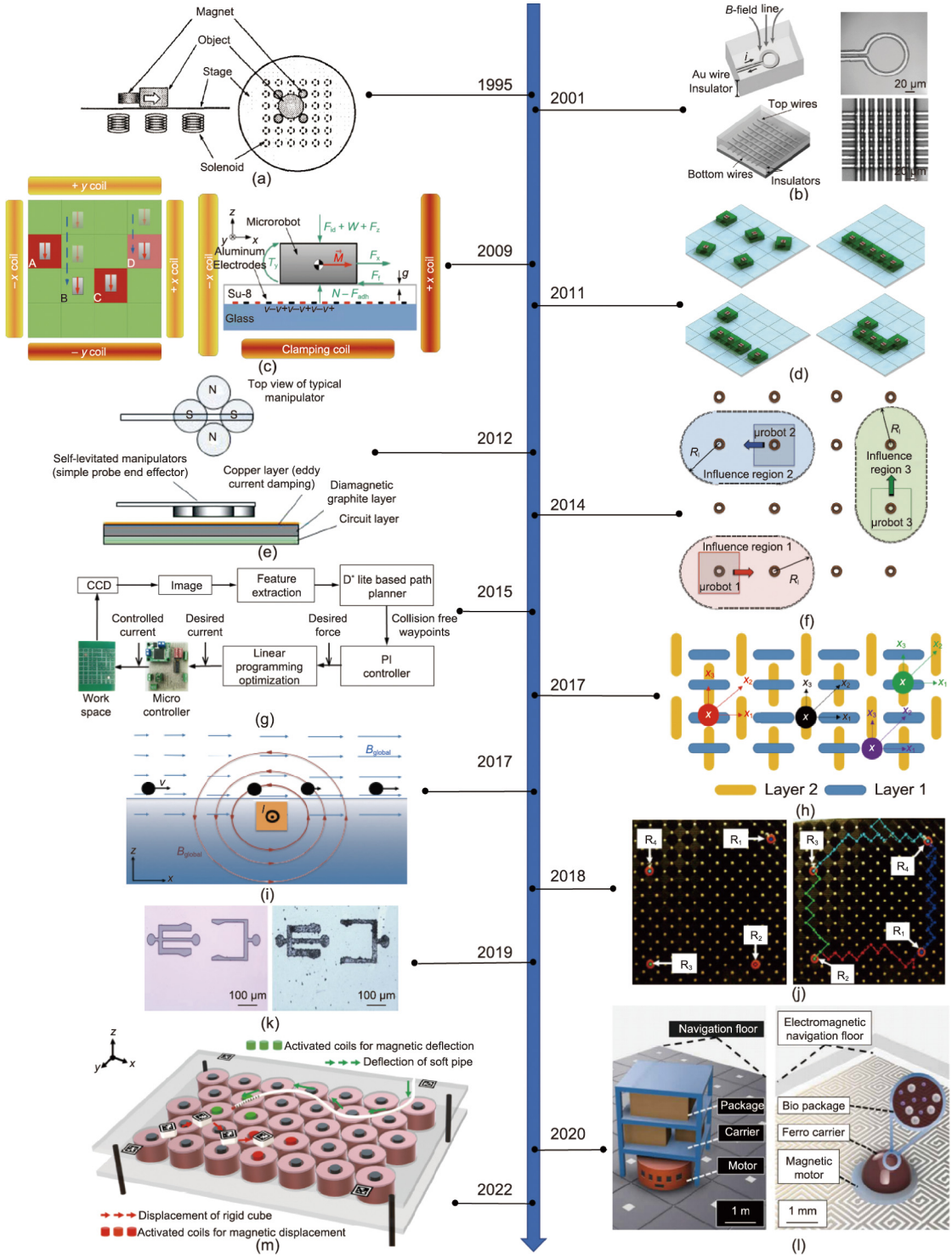

Fig. 6. The development of independent control methods via a local electromagnetic field from the perspectives of system manufacturing, multifunctional control strategies, and system intelligence. (a) The first demonstration of independent control using a local solenoid array; (b) an improved solenoid structure for particle trapping and actuation; (c) applying an electrostatic force to anchor targets; (d) the use of local anchoring for pattern programming; (e) using printed circuit board (PCB)-integrated coils to provide a local field; (f) independent control in an open-loop manner; (g) independent control targets in a closed-loop manner with real-time position feedback; (h) the use of orthogonal double-layer microcoils to enhance the local field; (i) a combination of global and local fields for target manipulation; (j) the use of independent control to complete sequential and temporal tasks; (k) the cooperative transportation of two magnetic individuals; (l) an intelligent micro-storage system for droplet manipulation; (m) the independent control of soft and rigid robots using a planar coil array. *i*: current; A, B, C, D: four microrobots; F_{id}: electrostatic anchoring force; *W*: weight; F_x, F_z: magnetic forces; F_f: static friction force; *N*: reactive normal force; T_y: magnetic torque; F_{adh}: adhesive force; $\vec{M}$: magnetization vector of the microrobot; *V*–, *V*+: relative voltage across the electrodes; R_l: radius of influence; CCD: charge coupled device; PI: proportional–integral; *x*: current state; x_1–x_3: transition state; *I*: current; B_{global}: global magnetic field; B_{local}: local variations in magnetic fields; *v*: velocity. R_1–R_4: four robots. (a) Reproduced from Ref. [54] with permission; (b) reproduced from Ref. [55] with permission; (c) reproduced from Ref. [63] with permission; (d) reproduced from Ref. [64] with permission; (e) reproduced from Ref. [56] with permission; (f) reproduced from Ref. [57] with permission; (g) reproduced from Ref. [58] with permission; (h) reproduced from Ref. [59] with permission; (i) reproduced from Ref. [60] with permission; (j) reproduced from Ref. [4] with permission; (k) reproduced from Ref. [61] with permission; (l) reproduced from Ref. [62] with permission; (m) reproduced from Ref. [65] with permission.

recent attempt of individual actuation using local magnetic field. The limitation of this methodology is that it relies on high-precision manufacturing of the substrate, and it cannot expand the operation space to 3D space. Although this method addresses the error accumulation problem, it is difficult to accurately move the target between two local units, due to the drastic changes in the magnetic field between neighboring actuation units.

As early as 1995, researchers started designing multi-micro-electromagnets systems to operate several permanent magnet targets (Fig. 6(a)) [54]. Subsequently, Lee et al. [55] designed two types of micro-electromagnets (a ring and a matrix trap) to attract and trap particles with a high magnetic density (about 0.1 T) and magnetic gradient (about 10^4 T·m^{-1}) in 2001 (Fig. 6(b)). With advances in integrated circuit technology, Pelrine et al. [56] fabricated micro coils into a printed circuit board (PCB) to generate local magnetic fields in order to manipulate multiple homogeneous millimeter-scale robots (Fig. 6(e)). Similarly, Cappelleri et al. [57] adopted a micro-electro-mechanical system (MEMS)-fabricated micro coils array to manipulate magnet robots (Fig. 6(f)).

Simulation and open-loop experiments have demonstrated the success of the distributed control of multiple robots in a planar workspace. In order to reduce error accumulation, Chowdhury et al. [58,66] developed closed-loop control strategies with visual feedback obtained from a charge coupled device (CCD) camera (Fig. 6(g)). In their works, the D* lite-based path planner was used for waypoint determination, and a linear programming optimization algorithm was applied to determine the current of each driving unit according to the required actuation force. To overcome the weak actuation force in the low magnetic flux region between two solenoids, the researchers proposed a modified double-layer orthogonal layout of micro coils; this double-layer configuration was then demonstrated to perform microassembly tasks (Fig. 6(h)) [59,67]. Steager et al. [60] proposed a fine-scale manipulation strategy with micrometer precision through the superposition of global and local fields (Fig. 6(i)). Long-distance transport was actuated by a global field, while substrate-patterned local microwires were used to produce a local magnetic force to trap selected particles. The use of a local electromagnetic array to complete sequential and temporal tasks was first reported in Ref. [4] (Fig. 6(j)). After that, in 2019, Chakravarthula et al. [61] designed two collaborative robots with a snap-fit joint structure to transfer cargo (Fig. 6(k)); the robots were controlled to open and close independently and were capable of working together. Recently, researchers also demonstrated the assembly of electronic material using a digital magnetic substrate [68].

The operation of multiple magnetic robots presents an intrinsic coupling problem between individuals. Johnson et al. [69] discussed the interactions between microrobots and suggested a minimal distance to ensure that the attraction force is smaller than the static friction. Recently, a selective droplet manipulation system with a navigation floor was proposed in Ref. [62]. This study was inspired by an automated guided vehicle system in an intelligent warehouse. As shown in Fig. 6(l) [62], the navigation floor is embedded with an array of electromagnetics for actuating a permanent magnet. A ferromagnetic droplet mixed with bio-packages can move on the electromagnetic substrate for cargo delivery. The same approach was adopted for reconfiguring ferrofluid droplet robots [70,71]. Aside from a micro electromagnetic array, another independent control technique is based on electrostatic anchoring. With this method, Pawashe et al. [63] developed a selective control strategy using four external electric magnetic coils for actuation and extra interdigitated electrodes under the substrate to selectively brake the microrobots in place (Fig. 6(c)). In another similar system, the navigation surface was divided into a grid of cells fabricated with electrodes to trap the magnetic microrobot using electrostatic force. Because of the high producibility, the selective control of microrobots on a localized substrate is also used for assembly and disassembly tasks [64]. Recently, Li et al. [65] developed a magnetic system with an electromagnetic array for steering soft and rigid robots (Fig. 6(m)). The system demonstrated the potential of controlling multiple rigid robots or cooperatively navigating multiple flexible robots.

3.4. Local moveable magnet strategies

The magnetic dipole model shows that a permanent magnet can generate a gradient field around it. This local magnetic field can be adjusted by repositioning the magnetic source and can be adopted to control the microrobot independently. Unlike actuation on a localized substrate, the method based on the movement of permanent magnets can be used to manipulate objects in a three-dimensional (3D) space, such as lifting and levitating targets in the workspace. However, the permanent-magnet-based method suffers from a high coupling effect for operating multiple objects. Moreover, the magnetic field cannot be turned off, which may introduce problems due to electromagnetic forces on other ferromagnetic objects.

Torres et al. [72,73] installed a conical permanent magnet on a robotic manipulator to act as an end-effector. The focusing magnetic field around the conical tip could be used to manipulate the target with increased accuracy (Fig. 7(a)) [72]. In 2015, Nelson and Abbott [74] demonstrated the simultaneous control of two magnetic screws with converging and diverging movement through a single rotating dipole. As shown in Fig. 7(b) [74], a rotational magnet can generate a rotational field that is in different directions at different regions. For example, for region A, the rotation axis is toward the right direction; for region B, it is toward the left direction. Thus, a rotating permanent magnet can be used to manipulate several objects toward different destinations. Subsequently, the same group further developed a closed-loop control model with position feedback and achieved a steady-state error below 0.2% and a ripple in the angular velocity below 1.0% [75]. A similar approach based on local magnetic actuation was used for the fine tilt-tuning of a laparoscopic tool [76]. Then, Ref. [77] completed multi-arm cooperation tasks using external moveable magnets (Fig. 7(c)). Modeling the magnetic gradient is challenging, especially when the material and morphology of the source magnetic field are un-uniform. Ref. [78] achieved the simultaneous and independent micromanipulation of two identical particles with the assistance of a neural network for modeling the magnetic flux density. Aside from solid materials, ferromagnetic fluidics have also been used for building multi-joint robots [79]. When external magnets were placed on certain joints, the local pressure increased and bent the joint due to the accumulation of ferromagnetic fluidics (Fig. 7(d)) [79]. Accordingly, different motion patterns were formed by actuating multiple joints independently. A similar mechanism has been adopted as a magnetorheological valve for the distributed control of soft robots [80].

3.5. Frequency resonate strategies

Frequency selection is another representative method for the selective control of multiple magnetic microrobots in the same external magnetic field. In this approach, the microrobots or agents are designed to have different resonance frequencies. Frequency-based methods can be roughly divided into three categories: ① microrobots fabricated with different materials or compositions, ② microrobots with specially designed structures or sizes, and ③ customized electronic circuits with different frequency characteristics.

Utilizing a step-out frequency is one of the most widely used methods for the selective control of multiple robots [81]. The step-out frequency is the maximum synchronized frequency

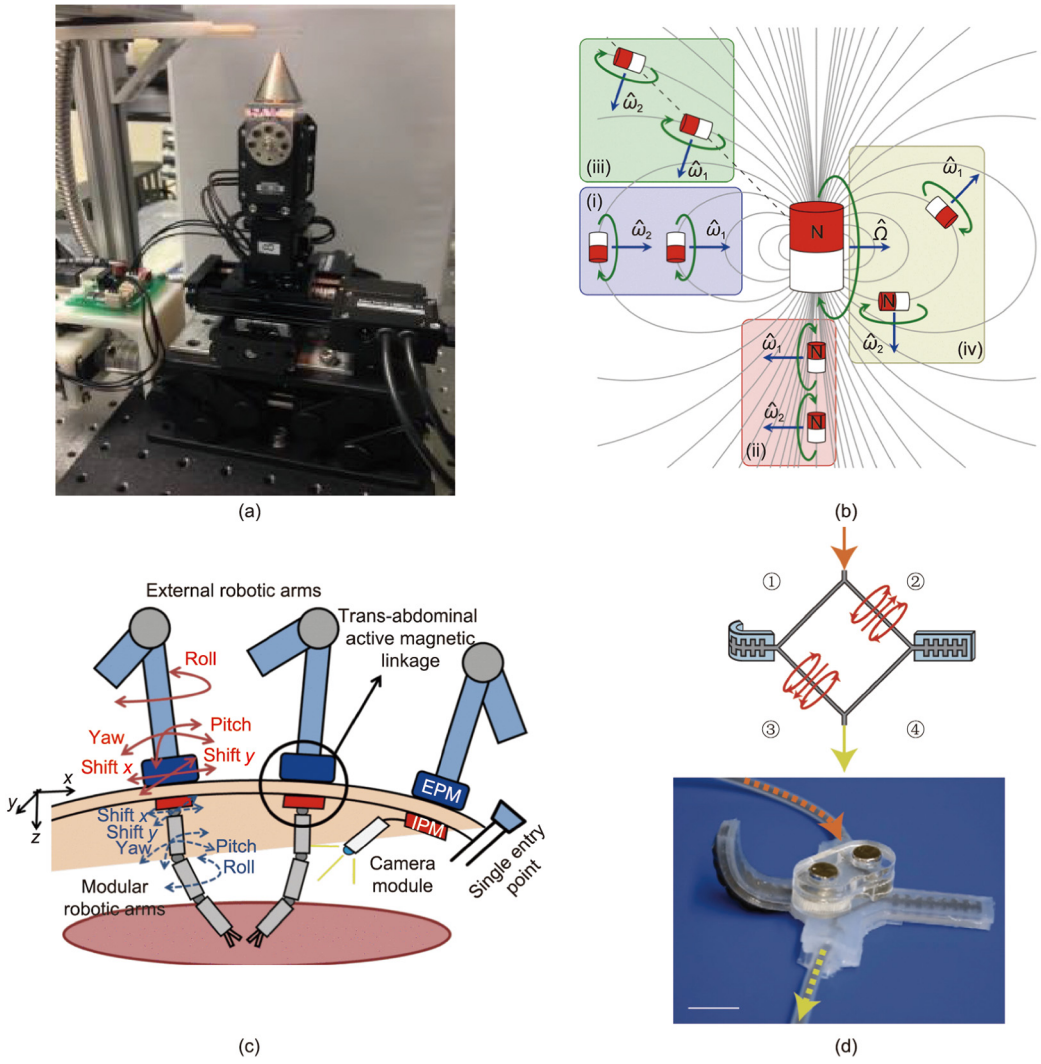

Fig. 7. Independent control by a local permanent magnet. (a) A conical permanent magnet is installed as the end-effector of a robot manipulator, which is used to generate a local magnetic field to manipulate devices; (b) a permanent magnet can generate torque in different directions with the same frequency at any two positions; (c) independent and cooperative operation of multi-arm robots driven by a local permanent magnet; (d) local permanent magnets cause magnetic fluid to gather and block, thereby independently controlling related arms. $\hat{\Omega}$, $\hat{\omega}_1$, $\hat{\omega}_2$: rotation axis; EPM: external permanent magnet; IPM: inner permanent magnet. (a) Reproduced from Ref. [72] with permission; (b) reproduced from Ref. [74] with permission; (c) reproduced from Ref. [77] with permission; (d) reproduced from Ref. [79] with permission.

corresponding to the externally applied field. When the external frequency is lower than all the individuals' step-out frequency, multiple robots can be actuated simultaneously. In contrast, if the external frequency is beyond the step-out frequency of a specific microrobot, then that microrobot will slow down or remain stationary, as the driving magnetic torque is smaller than the load torque of the microrobot.

In 2002, Ishiyama et al. [82] designed two micromachines by attaching permanent magnetic caps to screw tips. The two micromachines were designed with different lengths (6 mm vs 9 mm). The experiments showed that both machines exhibited a synchronized response to a field of 1 Hz. When the frequency was increased to 80 Hz, the micromachine with a greater length could still be actuated, but the shorter machine became stationary ((i) in Fig. 8(a)) [82]. In a subsequent study, the same group further investigated the independent orientation control of two micromachines [83]. Vach et al. [84] developed five micro-magnetic propellers with different frequency-speed characteristics and achieved selective control for independent steering ((ii) in Fig. 8(a)). Using the same strategy, Mahoney et al. [85] analyzed the different frequency responses of a soft ferromagnet and a permanent magnet. When the applied frequency was above the step-out frequency of two small devices, the researchers achieved differential speed control of two individuals ((iii) in Fig. 8(a)) [85]. The different frequency responses were also used for sorting magnetic micromachines [86]. Surface modification can also change the frequency response due to the distinct friction force. For example, Cheang et al. [87] applied a chemical binding method to combine three magnetic particles into a curved structure ((iv) in Fig. 8(a)). Although all the individuals had the same geometry and magnetic properties, the presence of hydrophilic or hydrophobic coating materials on the surface could cause the different friction to affect the individuals' swimming dynamics in the water. As a result, microswimmers with hydrophobic surfaces exhibited a higher step-out frequency than those with hydrophilic surfaces.

An individualized structure design is another strategy to modify the step-out frequency. A representative design can be seen in (i) in Fig. 8(b) [88]. In this case, the microrobot consisted of two nickel objects mounted on the substrate with a micro gap between them. The nickel bodies could be made to contract or expand by changing the direction of the external magnetic field. Anisotropic feet on the bottom of robot's bodies allowed net locomotion under a sequence

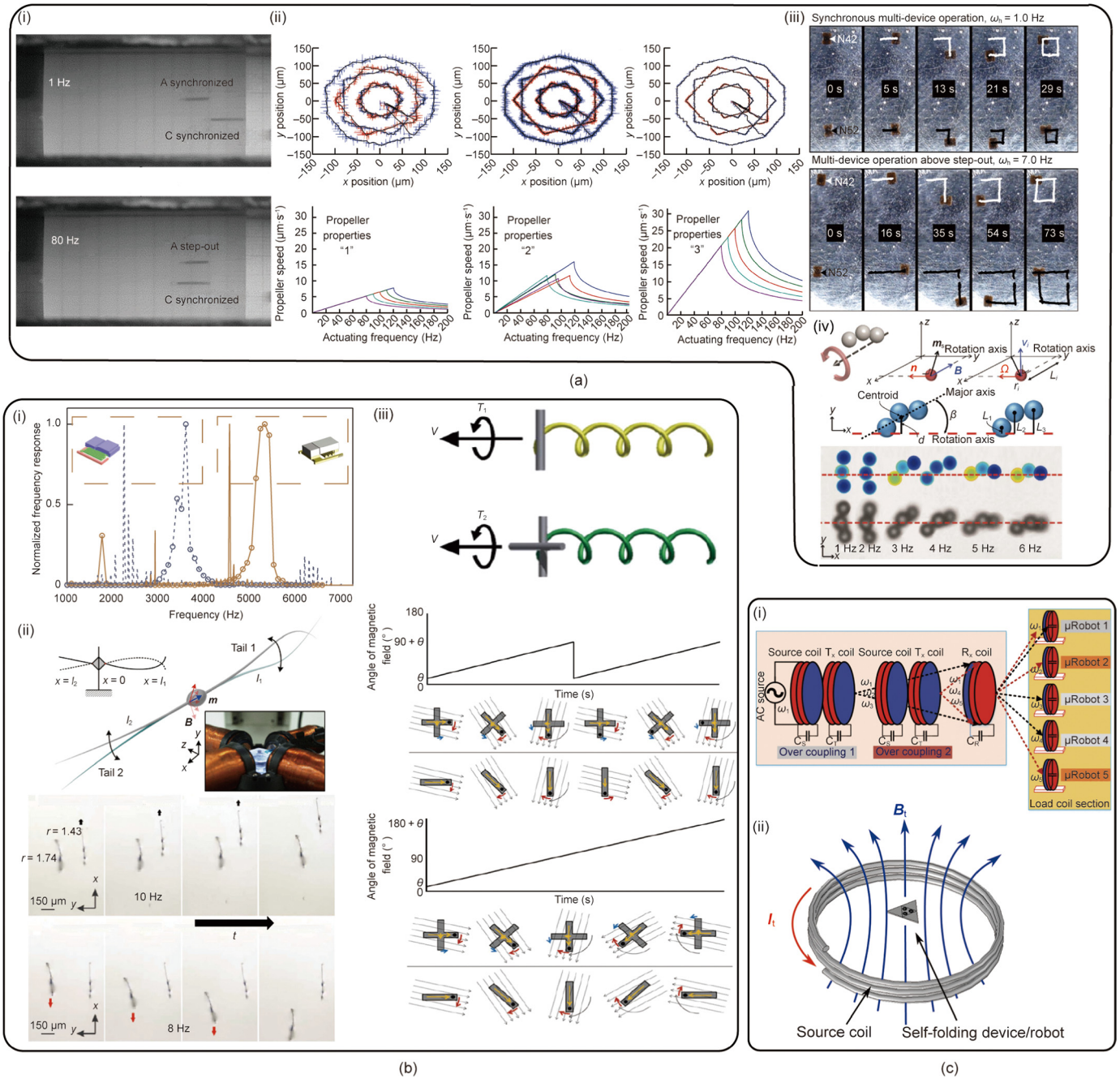

Fig. 8. Selective control via frequency resonance. (a) Inner properties caused different resonance frequencies: (i) different diameters and lengths for selective control; (ii) individuals with different materials can be controlled for independent trajectories; (iii) a distinct step-out frequency regulates the speed of controlled devices; (iv) the surface materials have different hydrophilic properties, resulting in different resonance frequencies. (b) A specialized structure caused different resonance frequencies: (i) Different installation modes result in different forces under an external magnetic field (each robot is embedded with two small magnets, one installed parallel to the axis and the other installed horizontally on the axis). The two embedded magnets can be made to attract or repel each other by adjusting the orientation of the external field, thus propelling the robot. (ii) Two-tailed sperm robot, where different length ratios of the two tails can result in a distinct step-out frequency; (iii) different head structures (bar-shaped head vs cross-shaped head) can result in different extended forces and resonance frequencies under the actuation of an external magnetic field. (c) The resistor–capacitance (RC) circuit caused different resonance frequencies: (i) Different small robots can be controlled separately by frequency decoupling via an RC circuit; (ii) a multi-arm origami robot is controlled independently by controlling the frequency of the external magnetic field, in which a resistance–inductor–capacitance (RLC) circuit with a different frequency response and shape memory alloy is installed in each arm. A, C: two magnetic individuals; ω_h: applied frequency; N42, N52: two kinds of magnetic materials; $\boldsymbol{m}_s$: magnetic moment vector; $\boldsymbol{B}$: magnetic field; $\boldsymbol{n}$: unit vector perpendicular to $\boldsymbol{m}_s$ and $\boldsymbol{B}$; Ω: moving direction; d: the distance from the robot to the rotational axis; β: the angle between rotational axis and locomotion direction; L_1–L_3: the distance from beads' center to the rotational axis; L_i: the distance from robot's center to the rotational axis; r_i: the vector position of the ith bead; v_i: the tangential velocity of the ith bead; l_1, l_2: length of two tails; r: the length ratio of two tails; v: velocity; T_1, T_2: magnetic torque for two robots; θ: the angle between the axis of symmetry and the external magnetic; T_X: transmitter; R_X: receiving; C_S, C_T, C_R: the capacitance of source coil, transmitter coil, and receiving coil; ω_1–ω_5: the resonance frequency of five individuals; AC: alternating current; $\boldsymbol{I}_t$: input current of external coil; $\boldsymbol{B}_t$: magnetic field on the self-folding device. (a) Reproduced from Refs. [82,84,85,87] with permission; (b) reproduced from Refs. [88,90,91] with permission; (c) reproduced from Refs. [92,93] with permission.

actuation. The variations in the gap between the two masses and the assembly direction granted them different frequency responses. By applying these design strategies, the researchers achieved selective control of a group of microrobots. This unique design and control frame enabled the team to win the RoboCup competitions in 2007 and 2009 [88,89].

Inspired by the swimming morphology of human sperm, Khalil et al. [90] designed a microrobot with two tails mounted in counter directions ((ii) in Fig. 8(b)). The researchers found that the non-identical tails could be used to steer the microrobot by controlling the frequency of the applied field. A critical reversal frequency exists to stop the movement of a selected robot when the propulsion force generated by the two tails is equal in magnitude but opposite in direction. The researchers demonstrated that the critical frequency depended on the length ratio of the two tails. Accordingly, the microrobots were fabricated with varied tail length ratios and were selectively controlled by changing the input frequency.

In another representative study, helical microrobots were fabricated with a different structure of the magnetic head (type I: bar-shaped, type II: cross-shaped; (iii) in Fig. 8(b)) [91]. In the case of a 90-degree rapid change with the applied rotational field, the type I robot could rotate following the applied field, while the type II robot remained stationary. Accordingly, the difference in head design caused a variation in the step-out frequency.

For a mesoscale robot, the electromagnetic coils can be trigged selectively by means of different resonance frequencies of customized resistance–inductor–capacitance (RLC) circuits. This technique has been used for the selective control of multiple magnetic microrobots as shown in Fig. 8(c) [92,93]. For example, a simultaneous wireless power transfer and actuation system was demonstrated in 2018 [92]. In this system, the power from the source coil was selectively transferred to receiver coils with specific frequencies. The load coils were mounted within microrobots with different resonant frequencies equal to split frequency values ((i) in Fig. 8(c)) [92]. Similarly, a multi-joint origami microrobot with addressable control capability was developed in Ref. [93]. In this work, the external source coil provided a time-varying magnetic field by changing the current frequency and amplitude. Each joint was built with a shape memory array and an RLC resonator with a unique resonance frequency. When the frequency of the external field matched the resonance frequency of a selected RLC circuit, the corresponding joint was activated. Multiple joints could also be folded simultaneously by rapidly switching among individual frequencies or superposing all frequencies signals together ((ii) in Fig. 8(c)) [93].

4. State-of-the-art applications

4.1. Biomimetic applications

Dexterous operations generally require the coordination of multiple joints or several robots. Therefore, applying a multi-arm robot is essential for completing assignments with multiple DoFs. A conventional multi-joint robot is bulky due to the large number of assembly components, such as heavy motors and gears, making it unsuitable for applications on a small scale. Magnetic microrobots address this limitation because they can be remotely controlled and require a small space. Fig. 9(a) [79,93–95] shows some biomimetic applications by selectively stimulating the robot's joints. For example, Boyvat et al. [93] designed a multi-joint robotic arm, in which each joint was composed of a shape memory alloy and a separate receiver coil. The joints could be actuated independently or simultaneously by changing the driving frequency of the external magnetic source ((i) in Fig. 9(a)) [93]. Another study reported a smart device that was a multi-layer origami robot [94]. Each layer module was composed of an origami structure covered with a permanent magnet. The stack layout accumulated the required rotation torque from the top to the bottom layer, and the origami structure served as the rotation limit. As a result, each layer was able to expand and collapse independently in response to a specific range of magnetic strengths generated by an external field. This prototype was demonstrated to build a Schmitt trigger by using the applied magnetic field as the input and digitizing the corresponding mechanical response as a digital output ((ii) in Fig. 9(a)) [94]. Inspired by the performance of blooming flowers, Mao et al. [95] designed a flower robot by integrating electromagnetic coils in the petals. The "flower petals" could be selectively or simultaneously activated by controlling the feeding current ((iii) in Fig. 9(a)) [95]. An attractive design of a multi-legged caterpillar robot was developed in Ref. [79]. As shown in (iv) in Fig. 9(a) [79], the robot was pressured by ferromagnetic fluid. For selective control, a permanent magnet could be placed above the selected channels to gather the fluid, thereby blocking the channels. As a result, the selective and coordinative control of multiple legs enabled the robot to move toward destinations.

4.2. Assembly and cargo transportation

Although single or swam magnetic microrobots have been well investigated and have demonstrated their capability for cargo delivery, logistic tasks involving multiple microrobots remain challenging. Addressing this question by means of selective and cooperative control brings substantial benefits for future applications, because multiple microrobots can provide increased load capacity and dexterous manipulation capability for specific targets. Microassembly is a representative application area that can adopt cooperative manipulation for microassembly tasks, as shown in (i) in Fig. 9(b) [4]. Both global and local fields have been used to assemble multiple targets into different patterns [4,30]. Another assembly task was achieved with the assistance of a local magnetic field [61]. In this work, two magnetic grippers were designed with a snap-fit structure for transferring wrapped cargo ((ii) in Fig. 9(b)) [61]. Local magnetic field actuation techniques have also been adopted for manipulating multiple droplets (e.g., dispensing, delivering, and sensing) ((iii) in Fig. 9(b)) [62]. Local electrostatic anchoring was also adopted for trapping selected targets in a global magnetic field and thereby accomplishing assembly patterns by actuating and anchoring the selected objects in place. Most assembly applications with independent control strategies strongly rely on local field manipulation on 2D and specialized substrates. Future research is anticipated to expand from 2D manipulation to 3D operations by controlling the global magnetic field.

4.3. Medical applications

Many robotics and sensory systems have demonstrated their potential in medical applications in recent years [96,97]. Among them, magnetic microrobots have demonstrated outstanding potential in biomedical applications due to their multiple advantages, which include the following: ① Biological tissues are nearly transparent to a magnetic field; ② a magnetic field does not rely on open space, and microrobots can be operated remotely in deep tissues; and ③ magnetic manipulation does not require physical connections or extra space for on-board battery and circuits on board. Due to the small scale of magnetic microrobots, they can pass through narrow chambers such as the gastrointestinal tract, bronchial ducts, and blood vessels. Fig. 9(c) [35,36,53,77] shows biomedical potential of multiple magnetic joints or microrobots using selective control strategies.

In 2012, Natali et al. [77] demonstrated the cooperative control of multi-arm magnetron robots for surgical operations ((i) in Fig. 9(c)). An internal magnet was controlled by a permanent magnet that was located above the abdominal tissue. The distance between the inner joints was ensured to be long enough to avoid the cross-talk effect. To clear blood clots for stroke patients by a robot moving in blood vessels, Lee et al. [36] developed a multifunctional magnetic robot in which each function could be selectively

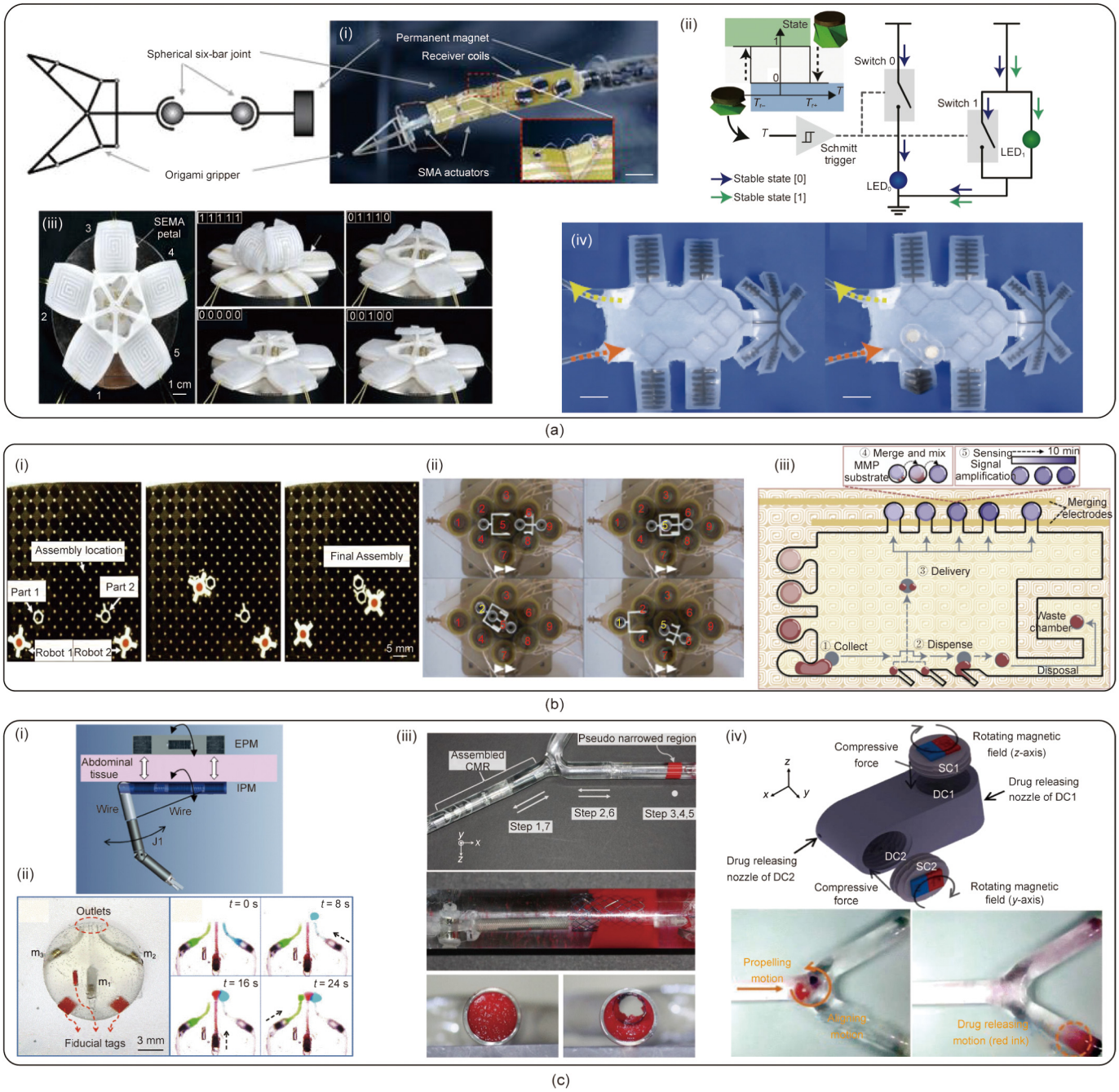

Fig. 9. State-of-the-art applications using the magnetic independent control method. (a) Multi-joint robots: (i) multi-joint robot arm; (ii) origami structure that realizes on–off control of the circuit; (iii) a flower with multiple petals; (iv) a multi-legged caterpillar robot. (b) Cargo delivery and assembly: (i) independent cargo transportation and assembly; (ii) two robots assembled to complete cargo transportation; (iii) droplet transport and manipulation. (c) Applications with medical potential: (i) surgical robotic arm; (ii) multifunctional (sample grab and drug delivery) capsule robot; (iii) crawling robot that removes blood clots; (iv) capsule robot with two chambers for sequential drug delivery. T_{r-}, T_{r+}: the required torques to fold and deploy the unit cell; T: magnetic torque; LED: light-emitting diode; SEMA: soft electromagnetic actuators; SMA: shape memory alloy; J1: joint 1; m_1–m_3: three magnetic robots; t: time; CMR: capsule magnetic robot; SC1, SC2: screws 1 and 2; DC1, DC2: drug channels 1 and 2. (a) Reproduced from Refs. [79,93–95] with permission; (b) reproduced from Refs. [4,61,62] with permission; (c) reproduced from Refs. [35,36,53,77] with permission.

activated ((iii) in Fig. 9(c)). Selective actuation of the magnetic microrobot was achieved by decoupling the motion of two orthogonal magnets.

Capsule microrobots have also been studied to diagnose and treat gastrointestinal diseases [98]. However, multifunctional capsule robots are underdeveloped, due to the limited workspace in millimeter or micrometer scales. Pioneering work in Ref. [35] presented a capsule robot with two orthogonal chambers to house different drugs ((ii) in Fig. 9(c)). The two chambers were embedded with magnets and could be independently controlled for the delivery of drugs to different locations. Another capsule robot was developed by integrating a three-DoF drug-releasing mechanism and a four-DoFs motion mechanism ((ii) in Fig. 9(c)) [53]. Shahrokhi et al. [46] used commercial MRI to actuate a magnetic microrobot for the independent control of navigation and biopsy. This robot consisted of two ferrous spheres; the sphere positioned on the plane pivoted for position control, while the other ferrous sphere was used to trigger the biopsy function.

5. Discussion and future perspective

According to the number of controllable devices, magnetic systems can be divided into three categories: individual systems, multi-device systems, and swarm systems. Independent control of a multi-device system is an effective strategy to increase load capacity and versatile functions. This review summarizes recent advances in independently controlling multiple microrobots through a magnetic field. The characteristics of the representative control strategies are summarized in Table 1 [4,21,28,29,35–38,42,44,54,62,64,74,77,79,83,86,89,90–92,96,99].

Among the previously mentioned five independent control strategies, the torque-based actuation method under a homogeneous magnetic field depends on the individual microrobots having different physical properties (e.g., variations in materials, geometry, or dimension). The propelling force generated by the gradient field can be programmed by analyzing kinematics models. It is essential to consider the feedback mechanism, because errors from nonlinear modeling can accumulate quickly when the gradient changes across various locations. Local solenoid actuation on a specialized substrate is often used to simplify the control problem and control a large number of microrobots independently. However, this strategy involves complicated fabrication and is confined to a 2D planar workspace. In contrast, microrobots based on permanent magnets are easy to fabricate and consume minimal energy. Nevertheless, undesired movement of the magnetic source may cause collisions or serious attraction problems, because the magnetic field cannot be turned off. Frequency resonance actuation is a popular actuation approach with independent control. This approach also relies on the different manufacturing of individual microrobots to give them a variety of frequency responses. A multi-device system with active coils has increased control flexibility because each onboard DoF can be easily actuated instead of being passively controlled by an external field. However, this category of magnetic systems is very bulky due to its manufacturing limitations, limiting its *in vivo* applications. The five mainstream strategies are sometimes combined to achieve a better actuation performance. For example, Khalesi et al. [100] achieved simultaneous and independent control of N magnetic robots by utilizing $2N$ permanent magnets and a pair of Helmholtz coils.

Although the reviewed studies have successfully demonstrated various technologies for the selective and independent control of multiple magnetic microrobots, increasing the actuation accuracy and the number of controllable robots is still challenging. Several

Table 1
Comparison of representative control strategies for independent magnetic microrobot control.

Control strategies	Sub-strategies	Magnetic source	Pros and cons	Application (representative)	Refs.
Uniform rotational field	Individuals have distinct magnetic properties	Helmholtz coil/permanent magnet	·Easy actuation ·Difficult to fabricate individuals in various magnetic composites	Drug delivery, swarm collaboration	[28,29]
	Individuals have novel physical design	Helmholtz coil/permanent magnet	·Easy actuation ·Difficult to design novel structures on a small scale	Biopsy and spray, medical examination	[35,36]
Global gradient field	Fully actuated system	Maxwell coil/commercial MRI/permanent magnet	·Individuals can have the same properties ·Specific kinematic model ·Precise position feedback is necessary	Biopsy and spray, trajectory following, medical examination	[21,37,38]
	Underactuated system	Maxwell coil/commercial MRI/permanent magnet	·Individuals can have the same properties ·Less magnetic source required ·Precise position feedback is necessary ·Require other external force to control	Biopsy and spray, trajectory following	[42,44]
Local magnetic field	Moveable permanent magnet	Permanent magnet	·Individuals can be of the same properties ·Precise position control ·Simple control system ·Difficult to control multiple objects simultaneously	Crawling robot, surgical robot	[74,77,79]
	Specialized substrate with micro solenoid array	Customized micro solenoid	·Multi-object simultaneous actuation ·Actuation errors will not exceed the distance between cells ·Limited in 2D space	Patterns programming, assembly and transfer, droplet manipulation	[4,54,62,64]
Frequency response	Individuals with different materials	Helmholtz coil/ customized coil array	·Easy actuation ·Require knowing the resonance frequency in advance ·Difficult to fabricate individuals with distinct properties	Drug delivery, swarm collaboration	[83,86]
	Individuals have a special designed structure or size	Helmholtz coil/ customized coil array	·Easy actuation ·Difficult to fabricate novel structures in the small structure	Swarm collaboration, medical examination	[90–92]
	Customized circuit with different frequency responses	Customized planar coil	·Easy fabrication ·Require electricity or thermal transfer ·Individuals are relatively bulky	Multi-joint robot, crawling robot, surgical robot	[89]
Active actuation	Individuals determine their own movement rather than being controlled by an external field	Permanent magnet	·More individuals can be actuated simultaneously ·Individuals are bulky	Multi-joint robot, crawling robot	[96,99]

critical solutions suggested below could be considered to achieve a higher level of dexterousness for controlling multiple microrobots:

- Establish a refined kinematic equation for multiple controlled microrobots in a magnetic field by considering electromagnetic, gravitational, adhesive, frictional, and fluid forces. The modeling of these forces is introduced in Refs. [101,102].
- Design a dexterous magnetic actuation system. In such a system, the magnetic density could be strengthened in a selected area for individual control of the target. Example systems with adjustable position and orientation of the electromagnetic sources are suggested in Refs. [22,103].
- Build an active magnetron system with numerous independently controlled devices. For example, the integration of soft microrobots with customized electromagnetic coils would enable the independent control of a high DoF system.
- Combine a magnetic system with other field-driven techniques (e.g., acoustic, light, and electrostatic). The use of an electrostatic force to selectively lock magnetic microrobots has been reported. Future research could be conducted to develop more reliable methods by combining a magnetic field with light or acoustic waves for micromanipulation in a 3D space. Several examples of multi-field combined controlling techniques are provided in Refs. [104,105].

Group control is significant in medical applications since a microrobot's size limits its drug delivery payload. Moreover, independent control of multiple robots is necessary to complete temporal tasks, such as drug delivery to multiple locations over a sustained period. The scales of most robots that can be independently controlled are in the micrometer to millimeter range. For these nanorobots, swarm control strategies may be more suitable in order to increase the payload capability, but achieving independent control is challenging. Furthermore, it is difficult to apply a larger-scale robot in medical applications due to the confined workspace. Previous research has successfully demonstrated the use of selective and independent control multi-joint magnetic systems for surgical operations, self-assembly, and drug delivery. The translational impact on clinical problems requires additional efforts to ensure high safety and reliability by conducting animal and physical experiments.

6. Conclusions

In summary, this survey reviewed multiple magnetic robotic systems that can be controlled independently and cooperatively for complicated manipulations. We first introduced the general magnetic coupling mechanisms and explained the state-of-art control strategies in five categories. The advantages and limitations of the methods in each category were reviewed. Applications of independent microrobots and of the selective control of multiple magnetic microrobots were discussed in three categories: multi-joint surgical robotic manipulation, cargo transportation, and biomedical treatment. A summary table including representative studies was provided, and critical challenges for future research were discussed. Although research on the selective and independent control of multiple magnetic microrobots still presents many challenges and is in its infancy, it has vast potential to transform robotic micromanipulation into real applications with increased dexterity and improved payload output. The ability to control each microrobot for a specialized task will elevate the microrobotic system to a high level of intelligence.

Acknowledgments

This work was supported by the Research Grant Council (RGC) of Hong Kong (11212321, 11217922, and ECS-21212720), Basic and Applied Basic Research Fund of Guangdong, China, and Science, Technology and Innovation Committee of Shenzhen (SGDX20210823104001011).

Compliance with ethics guidelines

Min Wang, Tianyi Wu, Rui Liu, Zhuoran Zhang, and Jun Liu declare that they have no conflict of interest or financial conflicts to disclose.

References

[1] Son D, Gilbert H, Sitti M. Magnetically actuated soft capsule endoscope for fine-needle biopsy. Soft Robot 2020;7(1):10–21.
[2] Polyak B, Friedman G. Magnetic targeting for site-specific drug delivery: applications and clinical potential. Expert Opin Drug Deliv 2009;6(1):53–70.
[3] Wang X, Ho C, Tsatskis Y, Law J, Zhang Z, Zhu M, et al. Intracellular manipulation and measurement with multipole magnetic tweezers. Sci Robot 2019;4(28):eaav6180.
[4] Kantaros Y, Johnson BV, Chowdhury S, Cappelleri DJ, Zavlanos MM. Control of magnetic microrobot teams for temporal micromanipulation tasks. IEEE Trans Robot 2018;34(6):1472–89.
[5] Rao KJ, Li F, Meng L, Zheng H, Cai F, Wang W. A force to be reckoned with: a review of synthetic microswimmers powered by ultrasound. Small 2015;11(24):2836–46.
[6] Palima D, Glückstad J. Gearing up for optical microrobotics: micromanipulation and actuation of synthetic microstructures by optical forces. Laser Photonics Rev 2013;7(4):478–94.
[7] Erdem EY, Chen YM, Mohebbi M, Suh JW, Kovacs GTA, Darling RB, et al. Thermally actuated omnidirectional walking microrobot. J Microelectromech Syst 2010;19(3):433–42.
[8] Karpelson M, Wei GY, Wood RJ. Driving high voltage piezoelectric actuators in microrobotic applications. Sens Actuators A Phys 2012;176:78–89.
[9] Kim Y, Parada GA, Liu S, Zhao X. Ferromagnetic soft continuum robots. Sci Robot 2019;4(33):eaax7329.
[10] Cui J, Huang TY, Luo Z, Testa P, Gu H, Chen XZ, et al. Nanomagnetic encoding of shape-morphing micromachines. Nature 2019;575(7781):164–8.
[11] Xie H, Sun M, Fan X, Lin Z, Chen W, Wang L, et al. Reconfigurable magnetic microrobot swarm: multimode transformation, locomotion, and manipulation. Sci Robot 2019;4(28):eaav8006.
[12] Mahoney AW, Abbott JJ. Five-degree-of-freedom manipulation of an untethered magnetic device in fluid using a single permanent magnet with application in stomach capsule endoscopy. Int J Robot Res 2015;35(1–3):129–47.
[13] Kummer MP, Abbott JJ, Kratochvil BE, Borer R, Sengul A, Nelson BJ. OctoMag: an electromagnetic system for 5-DOF wireless micromanipulation. IEEE Trans Robot 2010;26(6):1006–17.
[14] Yu J, Wang B, Du X, Wang Q, Zhang L. Ultra-extensible ribbon-like magnetic microswarm Nat Commun 2018;9(1):3260.
[15] Yu J, Jin D, Chan KF, Wang Q, Yuan K, Zhang L. Active generation and magnetic actuation of microrobotic swarms in bio-fluids. Nat Commun 2019;10(1):5631.
[16] Abbott JJ, Diller E, Petruska AJ. Magnetic methods in robotics. Annu Rev Control Robot Auton Syst 2020;3(1):57–90.
[17] Yang L, Zhang L. Motion control in magnetic microrobotics: from individual and multiple robots to swarms. Annu Rev Control Robot Auton Syst 2020;4(1):509–34.
[18] Cao Q, Han X, Li L. Configurations and control of magnetic fields for manipulating magnetic particles in microfluidic applications: magnet systems and manipulation mechanisms. Lab Chip 2014;14(15):2762–77.
[19] Hwang J, Kim J, Choi H. A review of magnetic actuation systems and magnetically actuated guidewire- and catheter-based microrobots for vascular interventions. Intell Serv Robot 2020;13(1):1–14.
[20] Alapan Y, Yasa O, Yigit B, Yasa IC, Erkoc P, Sitti M. Microrobotics and microorganisms: biohybrid autonomous cellular robots. Annu Rev Control Robot Auton Syst 2019;2(1):205–30.
[21] Ongaro F, Pane S, Scheggi S, Misra S. Design of an electromagnetic setup for independent three-dimensional control of pairs of identical and nonidentical microrobots. IEEE Trans Robot 2019;35(1):174–83.
[22] Du X, Zhang M, Yu J, Yang L, Chiu WYP, Zhang L. Design and real-time optimization for a magnetic actuation system with enhanced flexibility. IEEE/ASME Trans Mechatron 2020;26(3):1524–35.
[23] Cao Q, Fan Q, Chen Q, Liu C, Han X, Li L. Recent advances in manipulation of micro- and nano-objects with magnetic fields at small scales. Mater Horiz 2020;7(3):638–66.
[24] Xie H, Sun M, Fan X, Lin Z, Chen W, Wang L, et al. Reconfigurable magnetic microrobot swarm multimode transformation, locomotion, and manipulation. Sci Robot 2019;4(28):eaav8006.
[25] Yu J, Yang L, Zhang L. Pattern generation and motion control of a vortex-like paramagnetic nanoparticle swarm. Int J Robot Res 2018;37(8):912–30.

[26] Salehizadeh M, Diller E. Three-dimensional independent control of multiple magnetic microrobots via inter-agent forces. Int J Robot Res 2020;39 (12):1377–96.
[27] Zhang J, Salehizadeh M, Diller E. Parallel pick and place using two independent untethered mobile magnetic microgrippers. In: Proceedings of 2018 IEEE International Conference on Robotics and Automation (ICRA); 2018 May 21–25. Brisbane, QLD, Australia. IEEE; 2019. p. 123–8.
[28] Floyd S, Diller E, Pawashe C, Sitti M. Control methodologies for a heterogeneous group of untethered magnetic micro-robots. Int J Robot Res 2011;30(13):1553–65.
[29] Mandal P, Chopra V, Ghosh A. Independent positioning of magnetic nanomotors. ACS Nano 2015;9(5):4717–25.
[30] Tottori S, Zhang L, Peyer KE, Nelson BJ. Assembly, disassembly, and anomalous propulsion of microscopic helices. Nano Lett 2013;13(9):4263–8.
[31] Diller E, Floyd S, Pawashe C, Sitti M. Control of multiple heterogeneous magnetic micro-robots on non-specialized surfaces. In: Proceedings of 2011 IEEE International Conference on Robotics and Automation; 2011 May 9–13. Shanghai, China. IEEE; 2011. p. 115–20.
[32] Diller E, Floyd S, Pawashe C, Sitti M. Control of multiple heterogeneous magnetic microrobots in two dimensions on nonspecialized surfaces. IEEE Trans Robot 2012;28(1):172–82.
[33] Diller E, Miyashita S, Sitti M. Magnetic hysteresis for multi-state addressable magnetic microrobotic control. In: Proceedings of 2012 IEEE/RSJ International Conference on Intelligent Robots and Systems; 2012 Oct 7–12. Vilamoura-Algarve, Portugal. IEEE; 2012. p. 2325–31.
[34] Diller E, Miyashita S, Sitti M. Remotely addressable magnetic composite micropumps. RSC Adv 2012;2(9):3850–6.
[35] Choi K, Jang G, Jeon S, Nam J. Capsule-type magnetic microrobot actuated by an external magnetic field for selective drug delivery in human blood vessels. IEEE Trans Magn 2014;50(11):1–4.
[36] Lee W, Nam J, Jang B, Jang G. Selective motion control of a crawling magnetic robot system for wireless self-expandable stent delivery in narrowed tubular environments. IEEE Trans Ind Electron 2017;64(2):1636–44.
[37] Vartholomeos P, Akhavan-Sharif MR, Dupont PE. Motion planning for multiple millimeter-scale magnetic capsules in a fluid environment. In: Proceedings of 2012 IEEE International Conference on Robotics and Automation; 2012 May 14–18. Saint Paul, MN, USA. IEEE; 2012. p. 1927–32.
[38] Denise W, Wang J, Edward S, Vijay K. Control of multiple magnetic micro robots. In: Proceedings of ASME 2015 International Design Engineering Technical Conferences and Computers and Information in Engineering Conference; 2015 Aug 2–5. Boston, MA, USA. ASME; 2015. p. V004T09A041.
[39] Wong D, Steager EB, Kumar V. Independent control of identical magnetic robots in a plane. IEEE Robot Autom Lett 2016;1(1):554–61.
[40] Mellal L, Folio D, Belharet K, Ferreira A. Optimal control of multiple magnetic microbeads navigating in microfluidic channels. In: Proceedings of 2016 IEEE International Conference on Robotics and Automation (ICRA); 2016 May 16–21. Stockholm, Sweden. IEEE; 2016. p. 1921–6.
[41] Diller E, Giltinan J, Sitti M. Independent control of multiple magnetic microrobots in three dimensions. Int J Robot Res 2013;32(5):614–31.
[42] Kawaguchi T, Inoue Y, Ikeuchi M, Ikuta K. Independent actuation and master–slave control of multiple micro magnetic actuators. In: Proceedings of 2018 IEEE Micro Electro Mechanical Systems (MEMS); 2018 Jan 21–25. Belfast, UK. IEEE; 2018. p. 190–3.
[43] Shahrokhi S, Mahadev A, Becker AT. Algorithms for shaping a particle swarm with a shared input by exploiting non-slip wall contacts. In: Proceedings of 2017 IEEE/RSJ International Conference on Intelligent Robots and Systems (IROS); 2017 Sep 24–28. Vancouver, BC, Canada. IEEE; 2017. p. 4304–11.
[44] Becker A, Felfoul O, Dupont PE. Simultaneously powering and controlling many actuators with a clinical MRI scanner. In: Proceedings of 2014 IEEE/RSJ International Conference on Intelligent Robots and Systems; 2014 Sep 14–18. Chicago, IL, USA. IEEE; 2014. p. 2017–23.
[45] Denasi A, Misra S. Independent and leader–follower control for two magnetic micro-agents. IEEE Robot Autom Lett 2017;3(1):218–25.
[46] Shahrokhi S, Shi J, Isichei B, Becker AT. Exploiting nonslip wall contacts to position two particles using the same control input. IEEE Trans Robot 2019;35(3):577–88.
[47] Eqtami A, Felfoul O, Dupont PE. MRI-powered closed-loop control for multiple magnetic capsules. In: Proceedings of 2014 IEEE/RSJ International Conference on Intelligent Robots and Systems; 2014 Sep 14–18; Chicago, IL, USA. IEEE; 2014. p. 3536–42.
[48] Becker A, Ou Y, Kim P, Kim MJ, Julius A. Feedback control of many magnetized: tetrahymena pyriformis cells by exploiting phase inhomogeneity. In: Proceedings of 2013 IEEE/RSJ International Conference on Intelligent Robots and Systems; 2013 Nov 3–7. Tokyo, Japan. IEEE; 2013. p. 3317–23.
[49] Zhang J, Jain P, Diller E. Independent control of two millimeter-scale soft-bodied magnetic robotic swimmers. In: Proceedings of 2016 IEEE International Conference on Robotics and Automation (ICRA); 2016 May 16–21. Stockholm, Sweden. IEEE; 2016. p. 1933–8.
[50] Rahmer J, Stehning C, Gleich B. Spatially selective remote magnetic actuation of identical helical micromachines. Sci Robot 2017;2(3):eaal2845.
[51] Petruska AJ, Nelson BJ. Minimum bounds on the number of electromagnets required for remote magnetic manipulation. IEEE Trans Robot 2015;31 (3):714–22.
[52] Salmanipour S, Diller E. Eight-degrees-of-freedom remote actuation of small magnetic mechanisms. In: Proceedings of 2018 IEEE International Conference on Robotics and Automation (ICRA); 2018 May 21–25. Brisbane, QLD, Australia. IEEE; 2018. p. 3608–13.
[53] Salmanipour S, Youssefi O, Diller ED. Design of multi-degrees-of-freedom microrobots driven by homogeneous quasi-static magnetic fields. IEEE Trans Robot 2020;37(1):246–56.
[54] Inoue T, Iwatani K, Shimoyama I, Miura H. Micromanipulation using magnetic field. In: Proceedings of 1995 IEEE International Conference on Robotics and Automation; 1995 May 21–27. Nagoya, Japan. IEEE; 1995. p. 679–84.
[55] Lee CS, Lee H, Westervelt RM. Microelectromagnets for the control of magnetic nanoparticles. Appl Phys Lett 2001;79(20):3308–10.
[56] Pelrine R, Wong-Foy A, McCoy B, Holeman D, Mahoney R, Myers G, et al. Diamagnetically levitated robots: an approach to massively parallel robotic systems with unusual motion properties. In: Proceedings of 2012 IEEE International Conference on Robotics and Automation; 2012 May 14–18. Saint Paul, MN, USA. IEEE; 2012. p. 739–44.
[57] Cappelleri D, Efthymiou D, Goswami A, Vitoroulis N, Zavlanos M. Towards mobile microrobot swarms for additive micromanufacturing. Int J Adv Robot Syst 2014;11(9):150.
[58] Chowdhury S, Jing W, Cappelleri DJ. Towards independent control of multiple magnetic mobile microrobots. Micromachines 2015;7(1):3.
[59] Chowdhury S, Jing W, Cappelleri DJ. Designing local magnetic fields and path planning for independent actuation of multiple mobile microrobots. J Microbio Robot 2017;12(1–4):21–31.
[60] Steager E, Wong D, Wang J, Arora S, Kumar V. Control of multiple microrobots with multiscale magnetic field superposition. In: Proceedings of 2017 International Conference on Manipulation, Automation and Robotics at Small Scales (MARSS); 2017 Jul 17–21. Montreal, QC, Canada. IEEE; 2017. p. 1–6.
[61] Chakravarthula PN, Shekhar S, Ananthasuresh GK. Attachment, detachment, and navigation of small robots using local magnetic fields. In: Proceedings of 2019 International Conference on Manipulation, Automation and Robotics at Small Scales (MARSS); 2019 Jul 1–5. Helsinki, Finland. IEEE; 2019. p. 1–6.
[62] Yu W, Lin H, Wang Y, He X, Chen N, Sun K, et al. A ferrobotic system for automated microfluidic logistics. Sci Robot 2020;5(39):eaba4411.
[63] Pawashe C, Floyd S, Sitti M. Multiple magnetic microrobot control using electrostatic anchoring. Appl Phys Lett 2009;94(16):164108.
[64] Diller E, Pawashe C, Floyd S, Sitti M. Assembly and disassembly of magnetic mobile micro-robots towards deterministic 2D reconfigurable micro-systems. Int J Robot Res 2011;30(14):1667–80.
[65] Li X, Lu C, Song Z, Ding W, Zhang XP. Planar magnetic actuation for soft and rigid robots using a scalable electromagnet array. IEEE Robot Autom Lett 2022;7(4):9264–70.
[66] Chowdhury S, Jing WM, Jaron P, Cappelleri DJ. Path planning and control for autonomous navigation of single and multiple magnetic mobile microrobots. In: Proceedings of ASME 2015 International Design Engineering Technical Conferences and Computers and Information in Engineering Conference; 2015 Aug 2–5. Boston, MA, USA. ASME; 2015. p. V004T09A040.
[67] Chowdhury S, Jing W, Cappelleri DJ. Independent actuation of multiple microrobots using localized magnetic fields. In: Proceedings of 2016 International Conference on Manipulation, Automation and Robotics at Small Scales (MARSS); 2016 Jul 18–22. Paris, France. IEEE; 2016. p. 1–6.
[68] Lapuník V, Juřík M, Vítek M, Kuthan J, Mach F. Magnetically assembled electronic digital materials. In: Proceedings of 2022 International Conference on Manipulation, Automation and Robotics at Small Scales (MARSS); 2022 Jul 25–29. Toronto, ON, Canada. IEEE; 2022. p. 1–6.
[69] Johnson BV, Chowdhury S, Cappelleri DJ. Local magnetic field design and characterization for independent closed-loop control of multiple mobile microrobots. IEEE/ASME Trans Mechatron 2020;25(2):526–34.
[70] Fan X, Dong X, Karacakol AC, Xie H, Sitti M. Reconfigurable multifunctional ferrofluid droplet robots. Proc Natl Acad Sci USA 2020;117(45):27916–26.
[71] Zhang J, Wang X, Wang Z, Pan S, Yi B, Ai L, et al. Wetting ridge assisted programmed magnetic actuation of droplets on ferrofluid-infused surface. Nat Commun 2021;12(1):7136.
[72] Torres NA, Popa DO. Cooperative control of multiple untethered magnetic microrobots using a single magnetic field source. In: Proceedings of 2015 IEEE International Conference on Automation Science and Engineering (CASE); 2015 Aug 24–28. Gothenburg, Sweden. IEEE; 2015. p. 1608–13.
[73] Torres NA, Ruggeri S, Popa DO. Untethered microrobots actuated with focused permanent magnet field. In: Proceedings of ASME 2014 International Design Engineering Technical Conferences and Computers and Information in Engineering Conference; 2014 Aug 17–20. Buffalo, NY, USA. ASME; 2014. p. V004T09A024..
[74] Nelson ND, Abbott JJ. Generating two independent rotating magnetic fields with a single magnetic dipole for the propulsion of untethered magnetic devices. In: Proceedings of 2015 IEEE International Conference on Robotics and Automation (ICRA); 2015 May 26–30. Seattle, WA, USA. IEEE; 2015. p. 4056–61.
[75] Di Natali C, Buzzi J, Garbin N, Beccani M, Valdastri P. Closed-loop control of local magnetic actuation for robotic surgical instruments. IEEE Trans Robot 2015;31(1):143–56.
[76] Simi M, Pickens R, Menciassi A, Herrell SD, Valdastri P. Fine tilt tuning of a laparoscopic camera by local magnetic actuation: two-port nephrectomy experience on human cadavers. Surg Innov 2013;20(4):385–94.
[77] Natali CD, Ranzani T, Simi M, Menciassi A, Valdastri P. Trans-abdominal active magnetic linkage for robotic surgery: concept definition and model assessment. In: Proceedings of 2012 IEEE International Conference on

Robotics and Automation; 2012 May 14–18. Saint Paul, MN, USA. IEEE. p. 695–700.
[78] Isitman O, Kandemir H, Alcan G, Cenev Z, Zhou Q. Simultaneous and independent micromanipulation of two identical particles with robotic electromagnetic needles. In: Proceedings of International Conference on Manipulation, Automation and Robotics at Small Scales (MARSS); 2022 Jul 25–29. Toronto, ON, Canada. IEEE; 2022. p. 1–6.
[79] McDonald K, Rendos A, Woodman S, Brown KA, Ranzani T. Magnetorheological fluid-based flow control for soft robots. Adv Intell Syst 2020;2(11):2000139.
[80] Leps T, Glick PE, Ruffatto Iii D, Parness A, Tolley MT, Hartzell C. A low-power, jamming, magnetorheological valve using electropermanent magnets suitable for distributed control in soft robots. Smart Mater Struct 2020;29 (10):105025.
[81] Amoudruz L, Koumoutsakos P. Independent control and path planning of microswimmers with a uniform magnetic field. Adv Intell Syst 2021;4 (3):2100183.
[82] Ishiyama K, Sendoh M, Arai KI. Magnetic micromachines for medical applications. J Magn Magn Mater 2002;242:41–6.
[83] Sendoh M, Ishiyama K, Arai KI. Direction and individual control of magnetic micromachine. IEEE Trans Magn 2002;38(5):3356–8.
[84] Vach PJ, Klumpp S, Faivre D. Steering magnetic micropropellers along independent trajectories. J Phys D Appl Phys 2016;49(6):065003.
[85] Mahoney AW, Nelson ND, Peyer KE, Nelson BJ, Abbott JJ. Behavior of rotating magnetic microrobots above the step-out frequency with application to control of multi-microrobot systems. Appl Phys Lett 2014;104(14):144101.
[86] Howell TA, Osting B, Abbott JJ. Sorting rotating micromachines by variations in their magnetic properties. Phys Rev Appl 2018;9(5):054021.
[87] Cheang UK, Lee K, Julius AA, Kim MJ. Multiple-robot drug delivery strategy through coordinated teams of microswimmers. Appl Phys Lett 2014;105 (8):083705.
[88] Frutiger DR, Vollmers K, Kratochvil BE, Nelson BJ. Small, fast, and under control: wireless resonant magnetic micro-agents. Int J Robot Res 2009;29 (5):613–36.
[89] Kratochvil BE, Frutiger D, Vollmers K, Nelson BJ. Visual servoing and characterization of resonant magnetic actuators for decoupled locomotion of multiple untethered mobile microrobots. In: Proceedings of 2009 IEEE International Conference on Robotics and Automation; 2009 May 12–17. Kobe, Japan. IEEE; 2009. p. 2859–64.
[90] Khalil ISM, Tabak AF, Hamed Y, Tawakol M, Klingner A, Gohary NE, et al. Independent actuation of two-tailed microrobots. IEEE Robot Autom Lett 2018;3(3):1703–10.
[91] Tottori S, Sugita N, Kometani R, Ishihara S, Mitsuishi M. Selective control method for multiple magnetic helical microrobots. J Micro Nano Mech 2011;6 (3–4):89–95.
[92] Narayanamoorthi R, Juliet AV, Chokkalingam B. Frequency splitting-based wireless power transfer and simultaneous propulsion generation to multiple micro-robots. IEEE Sens J 2018;18(13):5566–75.
[93] Boyvat M, Koh JS, Wood RJ. Addressable wireless actuation for multijoint folding robots and devices. Sci Robot 2017;2(8):eaan1544.
[94] Novelino LS, Ze Q, Wu S, Paulino GH, Zhao R. Untethered control of functional origami microrobots with distributed actuation. Proc Natl Acad Sci USA 2020;117(39):24096–101.
[95] Mao G, Drack M, Karami-Mosammam M, Wirthl D, Stockinger T, Schwödiauer R, et al. Soft electromagnetic actuators. Sci Adv 2020;6(26). eabc0251.
[96] Libanori A, Chen G, Zhao X, Zhou Y, Chen J. Smart textiles for personalized healthcare. Nat Electron 2022;5(3):142–56.
[97] Chen G, Xiao X, Zhao X, Tat T, Bick M, Chen J. Electronic textiles for wearable point-of-care systems. Chem Rev 2022;122(3):3259–91.
[98] Wang M, Song S, Liu J, Meng MQH. Multipoint simultaneous tracking of wireless capsule endoscope using magnetic sensor array. IEEE Trans Instrum Meas 2021;70:1–10.
[99] Wang H, Rubenstein M. Autonomous mobile robot with independent control and externally driven actuation. In: Proceedings of 2016 IEEE/RSJ International Conference on Intelligent Robots and Systems (IROS); 2016 Oct 9–14. Daejeon, Republic of Korea. IEEE; 2016. p. 3647–52.
[100] Khalesi R, Yousefi M, Nejat Pishkenari H, Vossoughi G. Robust independent and simultaneous position control of multiple magnetic microrobots by sliding mode controller. Mechatronics 2022;84:102776.
[101] Pawashe C, Floyd S, Sitti M. Modeling and experimental characterization of an untethered magnetic micro-robot. Int J Robot Res 2009;28(8):1077–94.
[102] Floyd S, Pawashe C, Sitti M. Two-dimensional contact and noncontact micromanipulation in liquid using an untethered mobile magnetic microrobot. IEEE Trans Robot 2009;25(6):1332–42.
[103] Yang LD, Du XZ, Yu E, Jin DD, Zhang L. DeltaMag: an electromagnetic manipulation system with parallel mobile coils. In: Proceedings of 2019 International Conference on Robotics and Automation (ICRA); 2019 May 20–24. Montreal, QC, Canada. IEEE; 2019. p. 9814–20.
[104] Li C, Lau GC, Yuan H, Aggarwal A, Dominguez VL, Liu S, et al. Fast and programmable locomotion of hydrogel-metal hybrids under light and magnetic fields. Sci Robot 2020;5(49):eabb9822.
[105] Xu L, Gong D, Chen K, Cai J, Zhang W. Acoustic levitation applied for reducing undesired lateral drift of magnetic helical microrobots. J Appl Phys 2020;128 (18):184703.